Update of cross section measurement of $e^+e^- \to D_s^+ D_s^-$

Li Ke (like@ihep.ac.cn)

Yuan Changzheng, Huang Xingtao, Lou Xinchou

Outline

- Previous results
- Updates
- Extract signal yield
- Cross sections
- Summary

Previous results of Born cross sections

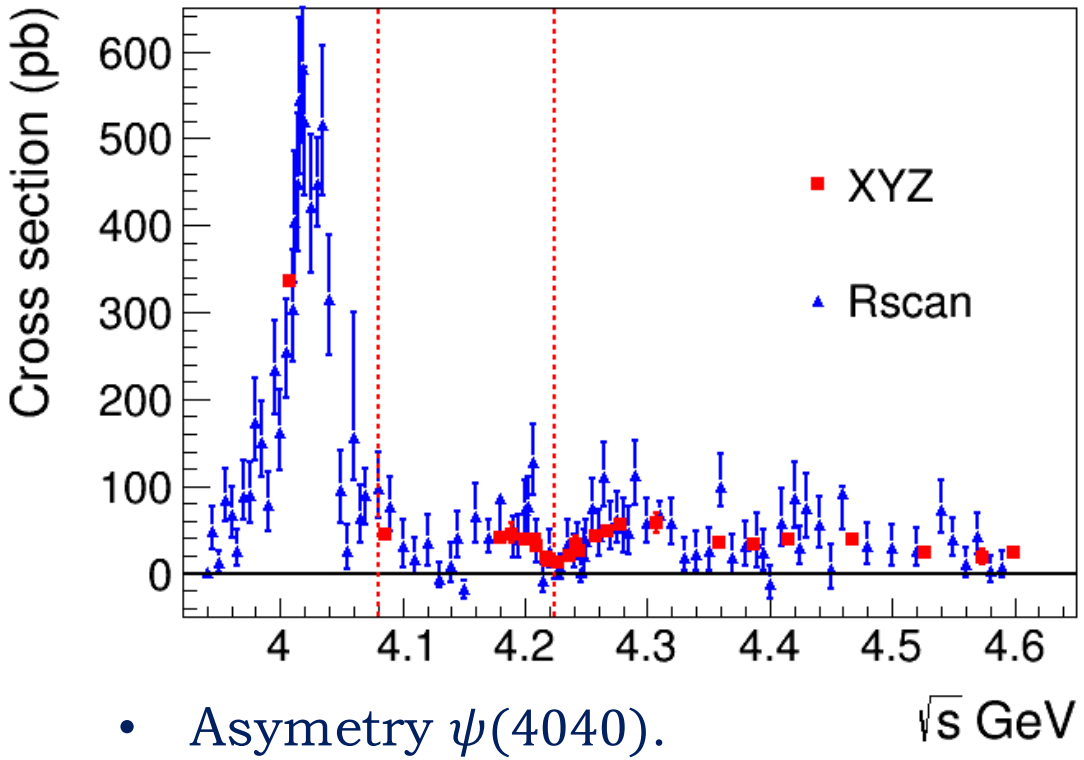

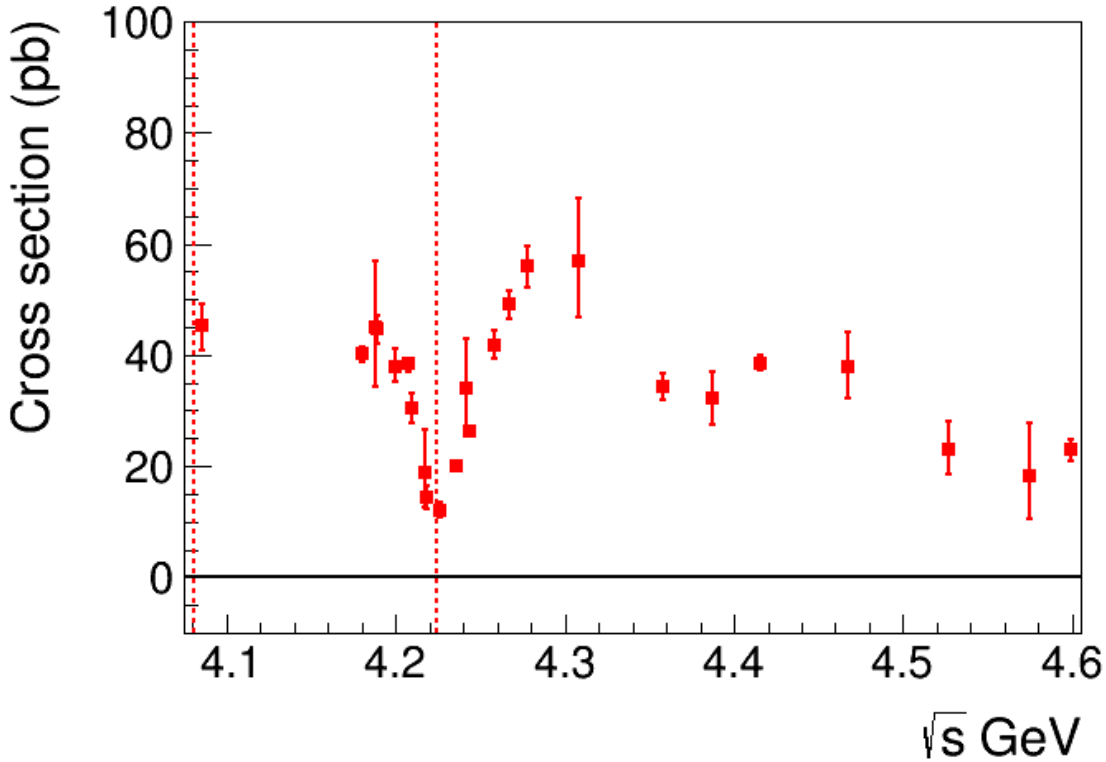

- Asymetry $\psi(4040)$.
- Dip at 4.22 GeV, just at the threshold of $D_s^* D_s^*$
- Cross section goes down at 4.31 GeV then goes up at 4.42 GeV.
- The dip could be caused by interference between Y(4260), $\psi(4160)$ and other states, or the threshold effect of $D_s^* D_s^*$. Unlike the $f_0(980)$, the cross section decrease below the threshold of $D_s^* D_s^*$ and has minimum value at the threshold.

Born cross sections

- Numbers are listed here

$\sqrt{s}$ (MeV)	σ^B (pb)	$\sqrt{s}$ (MeV)	σ^B (pb)
4008	$335.3^{+7.0}_{-7.0} \pm 2.2$	4085	$45.4^{+3.8}_{-4.5} \pm 0.0$
4189	$45.0^{+12.0}_{-10.7} \pm 1.5$	4208	$38.4^{+-1.3}_{-1.3} \pm 2.6$
4217	$18.9^{+7.5}_{-6.5} \pm 1.6$	4226	$12.1^{+1.4}_{-1.3} \pm 1.2$
4242	$34.0^{+9.0}_{-8.0} \pm 3.0$	4258	$41.8^{+2.5}_{-2.4} \pm 3.2$
4308	$57.0^{+11.2}_{-10.1} \pm 6.9$	4358	$34.2^{+2.3}_{-2.3} \pm 0.3$
4387	$32.3^{+4.8}_{-4.7} \pm 0.4$	4416	$38.6^{+1.4}_{-1.4} \pm 1.9$
4467	$38.0^{+6.1}_{-5.7} \pm 1.1$	4527	$23.1^{+4.9}_{-4.5} \pm 1.0$
4574	$18.3^{+9.3}_{-7.7} \pm 0.6$	4600	$22.9^{+2.1}_{-2.0} \pm 0.7$
4180	$40.1^{+1.3}_{-1.3} \pm 0.3$	4189	$44.6^{+2.7}_{-2.6} \pm 1.6$
4200	$38.0^{+3.1}_{-3.0} \pm 2.0$	4210	$30.5^{+2.8}_{-2.6} \pm 2.2$
4129	$14.4^{+2.1}_{-2.0} \pm 0.9$	4236	$20.2^{+0.4}_{-0.6} \pm 1.9$
4244	$26.2^{+1.0}_{-1.1} \pm 2.3$	4267	$49.1^{+2.6}_{-2.5} \pm 1.5$
4278	$56.0^{+3.7}_{-3.8} \pm 1.3$		

$\sqrt{s}$ (MeV)	σ^B (pb)	$\sqrt{s}$ (MeV)	σ^B (pb)		
3940	$0.2^{+5.7}_{-0.9} \pm 0.0$	3945	$47.4^{+29.7}_{-20.4} \pm 2.0$	3950	$11.5^{+14.1}_{-10.1} \pm 0.3$
3955	$85.1^{+35.1}_{-25.6} \pm 2.3$	3960	$66.3^{+32.4}_{-25.4} \pm 1.9$	3965	$26.2^{+24.6}_{-16.8} \pm 0.8$
3970	$88.8^{+40.7}_{-27.6} \pm 2.6$	3975	$89.4^{+38.6}_{-31.1} \pm 2.6$	3980	$173.5^{+51.8}_{-43.9} \pm 5.0$
3985	$150.4^{+48.2}_{-40.5} \pm 3.9$	3990	$78.7^{+37.2}_{-29.5} \pm 1.8$	3995	$233.2^{+57.9}_{-50.1} \pm 4.8$
4000	$161.0^{+51.0}_{-43.1} \pm 2.9$	4005	$254.4^{+60.7}_{-52.9} \pm 5.4$	4010	$303.9^{+68.9}_{-60.6} \pm 2.1$
4012	$404.9^{+80.1}_{-71.3} \pm 7.4$	4014	$448.1^{+82.1}_{-78.2} \pm 13.5$	4016	$544.9^{+94.8}_{-85.2} \pm 30.0$
4018	$580.6^{+93.9}_{-85.1} \pm 46.4$	4020	$519.5^{+62.4}_{-84.2} \pm 54.4$	4025	$420.6^{+84.5}_{-75.2} \pm 49.9$
4030	$447.0^{+52.9}_{-49.3} \pm 59.2$	4035	$515.6^{+90.5}_{-81.5} \pm 65.3$	4040	$314.8^{+73.8}_{-64.7} \pm 38.0$
4050	$95.4^{+46.0}_{-37.3} \pm 8.9$	4055	$26.0^{+30.4}_{-22.1} \pm 2.0$	4060	$156.4^{+143.7}_{-48.8} \pm 9.8$
4065	$64.4^{+37.7}_{-29.6} \pm 3.8$	4070	$89.1^{+30.4}_{-33.1} \pm 5.0$	4080	$97.4^{+41.2}_{-33.9} \pm 3.1$
4090	$76.4^{+35.0}_{-28.7} \pm 0.6$	4100	$30.4^{+30.4}_{-23.5} \pm 0.7$	4110	$16.0^{+25.4}_{-17.4} \pm 0.6$
4120	$34.6^{+32.4}_{-25.6} \pm 1.0$	4130	$-6.1^{+18.5}_{-10.4} \pm 0.1$	4140	$8.5^{+25.8}_{-18.5} \pm 0.2$
4145	$41.1^{+30.2}_{-22.8} \pm 1.4$	4150	$-18.6^{+11.0}_{-10.5} \pm 0.8$	4160	$65.6^{+37.0}_{-29.6} \pm 2.9$
4170	$40.6^{+20.1}_{-16.9} \pm 1.9$	4180	$86.9^{+3.4}_{-41.5} \pm 0.2$	4190	$43.4^{+22.6}_{-25.2} \pm 1.6$
4195	$39.2^{+28.9}_{-21.8} \pm 1.8$	4200	$72.5^{+34.5}_{-28.1} \pm 4.0$	4203	$75.9^{+35.2}_{-30.8} \pm 4.6$
4206	$127.2^{+44.5}_{-37.6} \pm 8.3$	4210	$32.8^{+27.8}_{-20.9} \pm 2.4$	4215	$-8.1^{+18.2}_{-14.1} \pm 0.7$
4220	$25.0^{+24.7}_{-19.3} \pm 2.3$	4225	$-0.6^{+10.1}_{-5.1} \pm 0.1$	4230	$5.2^{+17.2}_{-10.9} \pm 0.5$
4235	$33.7^{+27.3}_{--27.3} \pm 3.2$	4240	$22.6^{+22.3}_{-15.2} \pm 2.0$	4243	$32.4^{+26.1}_{-12.7} \pm 2.9$
4245	$0.8^{+26.1}_{-11.8} \pm 0.1$	4248	$20.7^{+29.0}_{-23.2} \pm 1.7$	4250	$36.2^{+25.9}_{-19.6} \pm 3.0$
4255	$74.6^{+33.5}_{-27.1} \pm 5.9$	4260	$42.9^{+29.8}_{-23.9} \pm 2.7$	4265	$110.8^{+40.0}_{-33.6} \pm 3.0$
4270	$52.1^{+30.8}_{-24.4} \pm 0.4$	4275	$61.5^{+32.4}_{-26.2} \pm 2.7$	4280	$51.6^{+33.7}_{-27.9} \pm 4.0$
4285	$46.8^{+30.6}_{-24.6} \pm 5.3$	4290	$112.1^{+39.7}_{-33.8} \pm 12.9$	4300	$57.1^{+28.9}_{-22.5} \pm 6.8$
4310	$66.5^{+15.1}_{--13.5} \pm 7.7$	4320	$57.1^{+29.2}_{-24.1} \pm 5.2$	4330	$18.8^{+21.4}_{-15.2} \pm 1.2$
4340	$22.3^{+26.2}_{-18.7} \pm 0.8$	4350	$25.2^{+27.2}_{-21.7} \pm 0.3$	4360	$99.9^{+37.9}_{-23.4} \pm 0.7$
4370	$18.9^{+25.5}_{-20.1} \pm 0.0$	4380	$30.8^{+28.6}_{-22.7} \pm 0.2$	4390	$35.0^{+33.8}_{-27.4} \pm 0.5$
4395	$22.9^{+26.4}_{-20.0} \pm 0.5$	4400	$-11.5^{+20.3}_{-17.5} \pm 0.3$	4410	$58.1^{+40.1}_{-26.8} \pm 2.5$
4420	$86.1^{+40.9}_{-34.2} \pm 4.1$	4425	$28.7^{+26.1}_{-19.2} \pm 1.3$	4430	$74.2^{+41.2}_{-33.8} \pm 3.3$
4440	$55.3^{+32.3}_{-25.7} \pm 2.3$	4450	$4.6^{+28.2}_{-23.2} \pm 0.2$	4460	$91.1^{+8.0}_{-40.8} \pm 2.9$
4480	$30.7^{+26.7}_{-20.2} \pm 1.2$	4500	$28.8^{+27.3}_{-20.5} \pm 1.6$	4520	$25.4^{+25.8}_{-17.4} \pm 1.2$
4540	$73.6^{+32.5}_{-27.0} \pm 3.1$	4550	$39.3^{+24.2}_{-19.2} \pm 1.6$	4560	$10.1^{+19.0}_{-14.6} \pm 0.4$
4570	$42.5^{+27.0}_{-21.3} \pm 1.5$	4580	$3.8^{+16.2}_{-14.7} \pm 0.1$	4590	$6.8^{+18.1}_{-12.0} \pm 0.2$

Updates

- Generator: KKMC -> ConExc
- Fit method: 1D fit -> 2D fit

2D plot of $M(D_s)$ vs. $RM(D_s)$

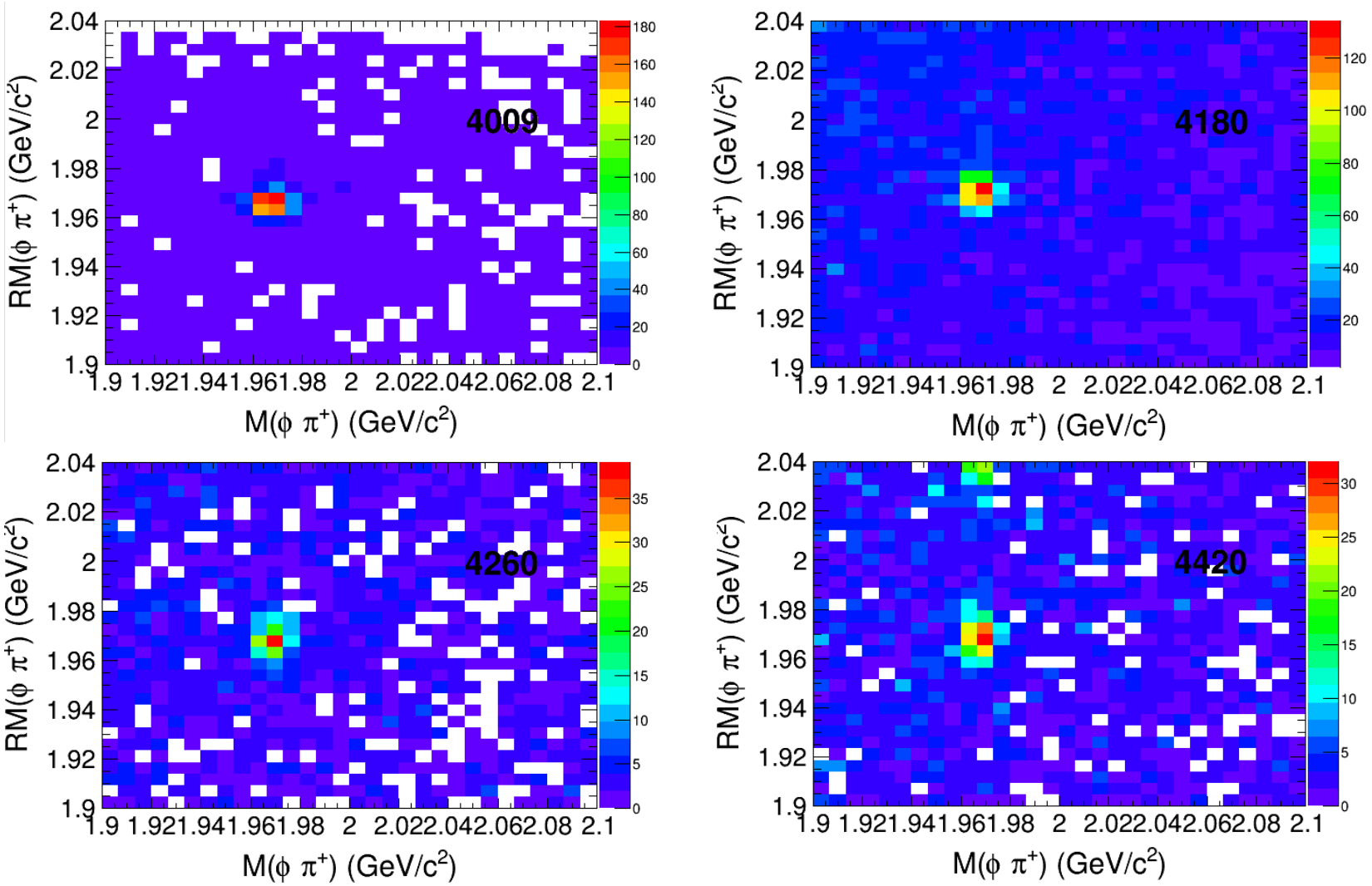

Background which has real D_s ($D_s^* D_s, D_s^* D_s^*$) is far way from signal region.

All background at signal region are $non - D_s$ events

Difference in mass between data and MC simulation

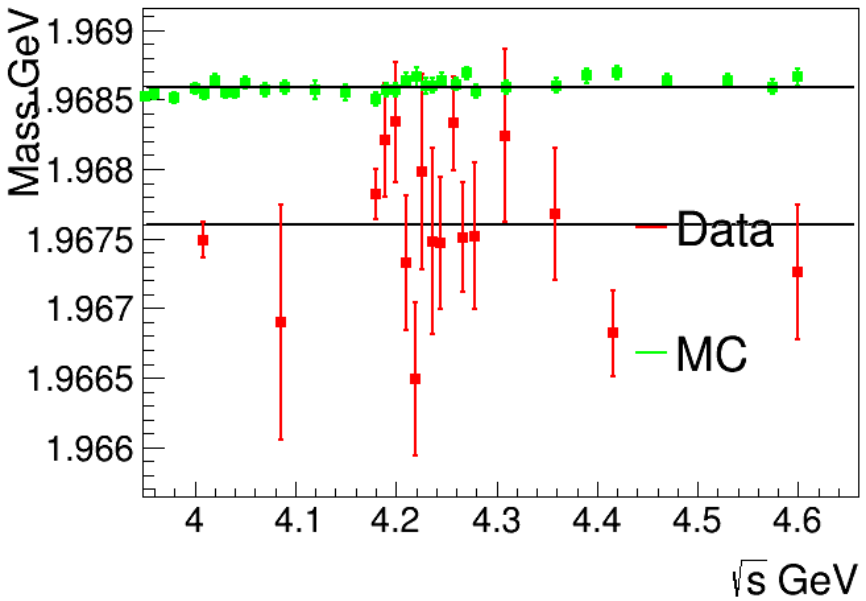

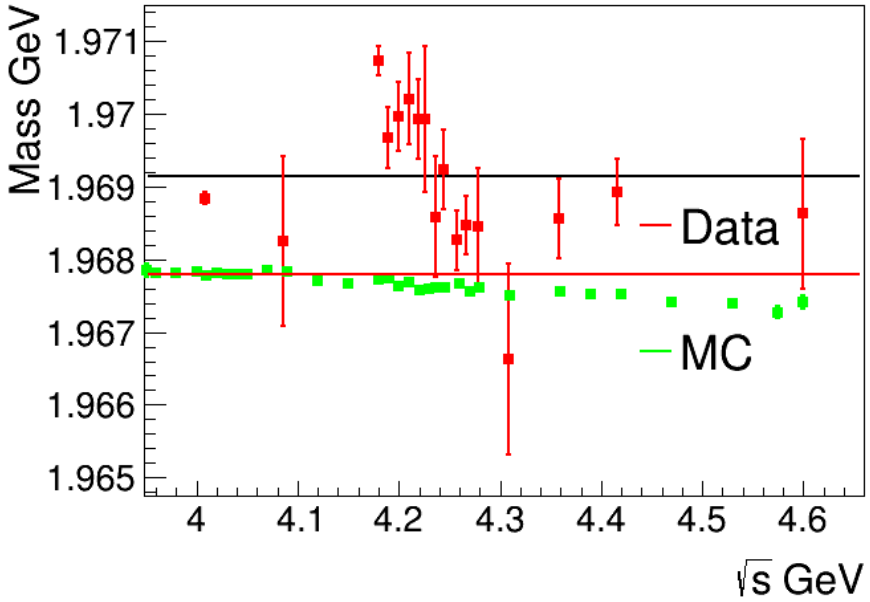

Fit the 1D invariant and recoil mass distribution of $\phi\pi$ and compare the difference .

Invariant mass ΔM: no big difference between difference energies.

Recoil massΔRM: related with ISR and energy calibration.

Difference in resolution between data and MC simulation

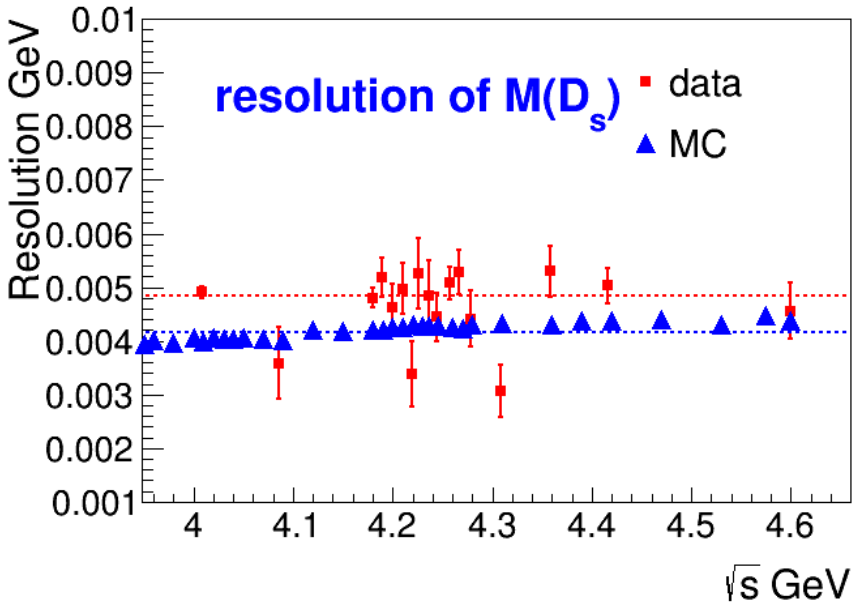

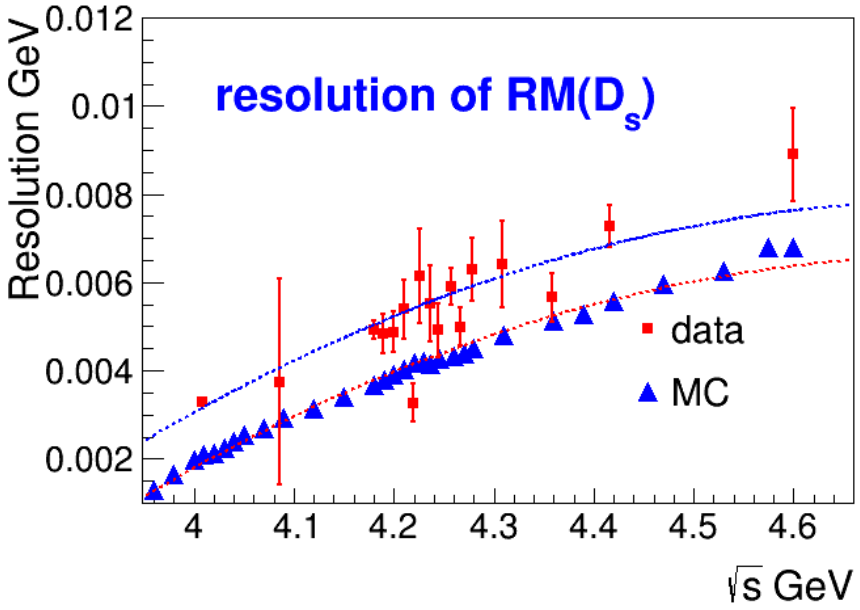

Fit the 1D distribution to get the mass resolution.

Systematic difference ($\Delta\sigma_M$ $\Delta\sigma_{RM}$) between data and MC around 1 MeV.

Difference in resolution between data and MC simulation

MC correction:

For each event, generate a set of random numbers following Gaussion distribution.

$$G(\Delta M, \Delta\sigma_M) \text{ and } G(\Delta RM, \Delta\sigma_{RM})$$

Correct the invariant and recoil mass of $\phi\pi$:

$$M(\phi\pi)_c = M(\phi\pi) + G(\Delta M, \Delta\sigma_M)$$
$$RM(\phi\pi)_c = RM(\phi\pi) + G(\Delta RM, \Delta\sigma_{RM})$$

Then use the 2D distribution to generate a PDF.

Background

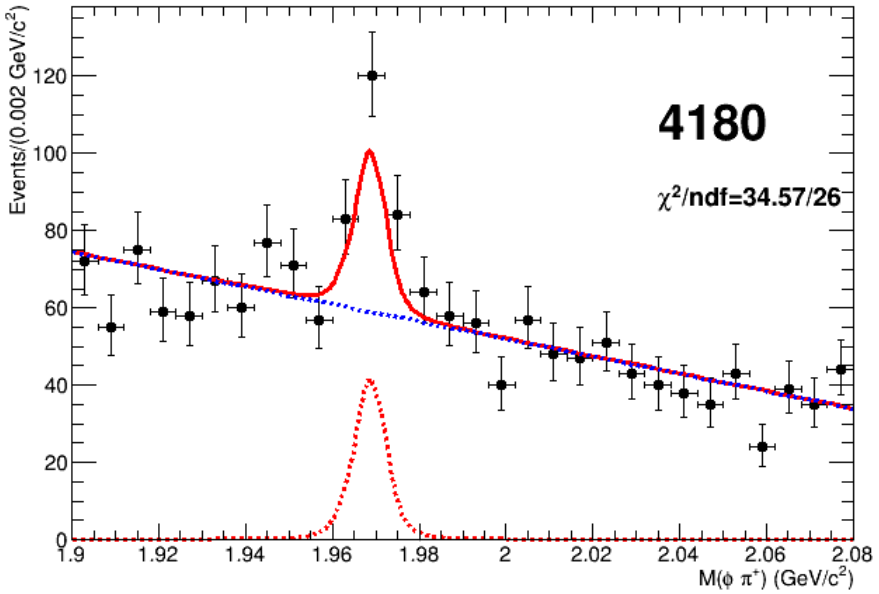

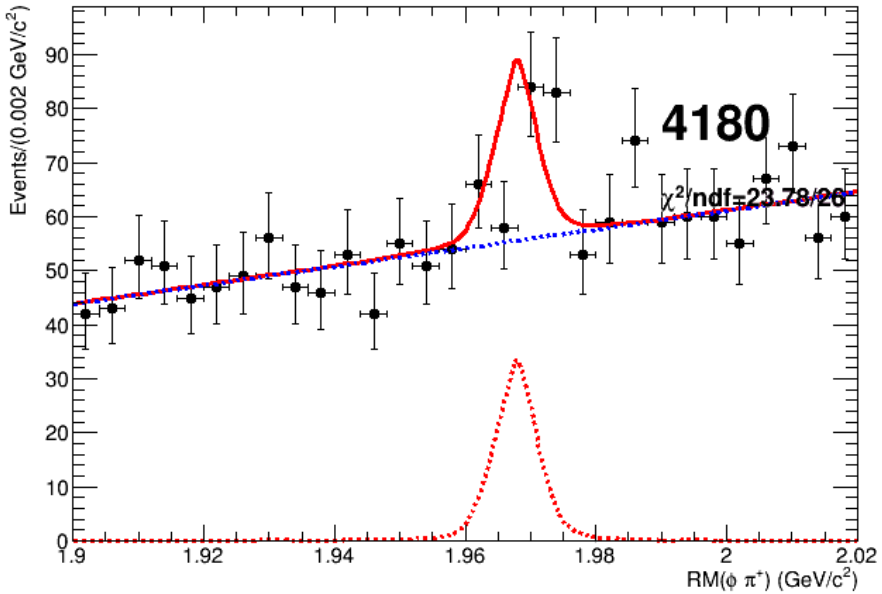

Test 2D fit with inclusive MC at 4180 MeV.

Signal: MC simulation with mass and resolution corrections.

Background: the product of two 1D 1-order polynomial function with no correlation.

Match well for the background events.

2D fit results: 4009 (top) and 4180 (bottom)

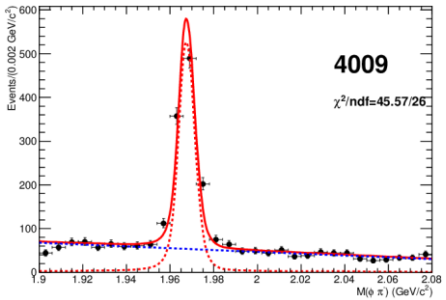

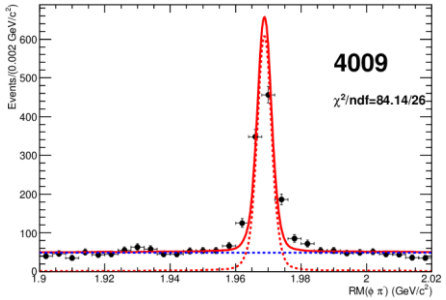

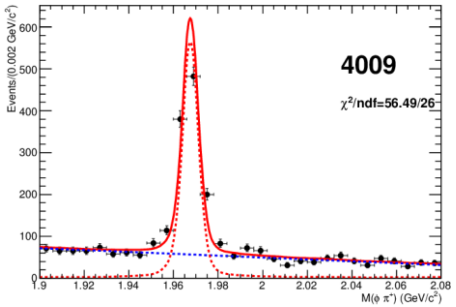

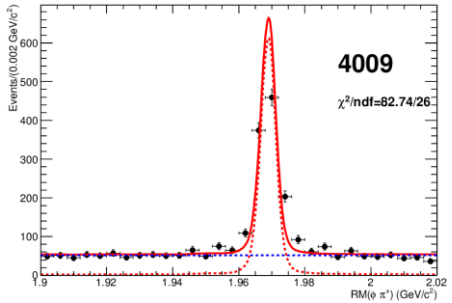

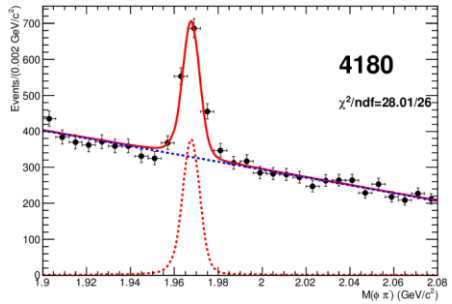

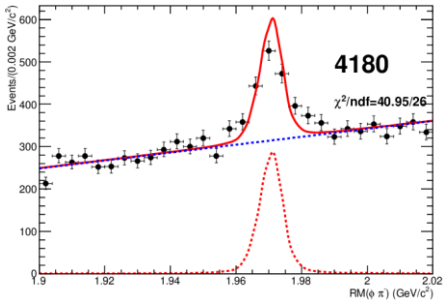

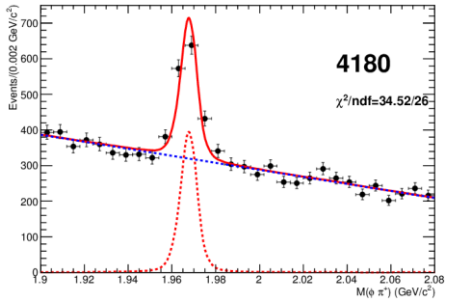

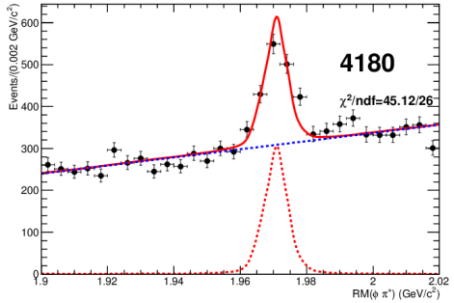

2D fit results: 4220 (top) and 4260 (bottom)

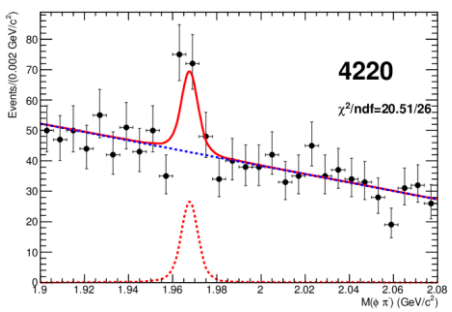

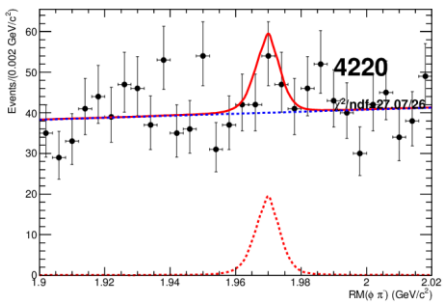

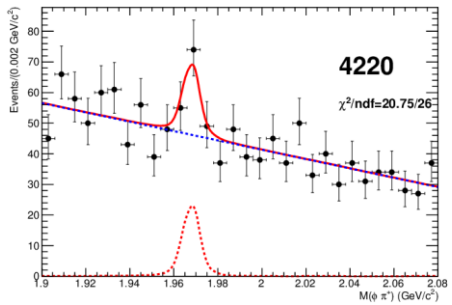

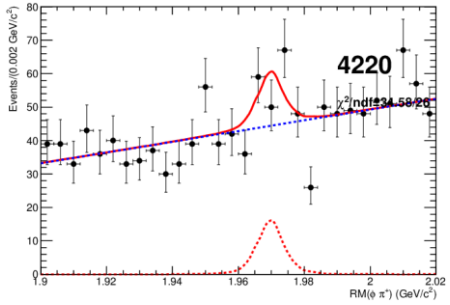

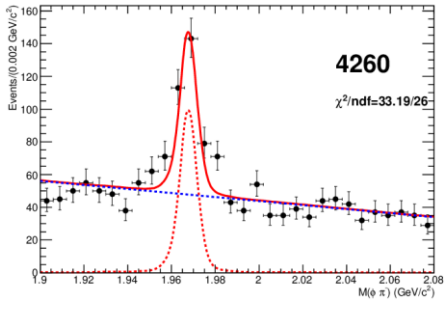

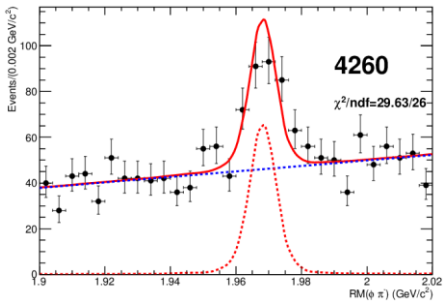

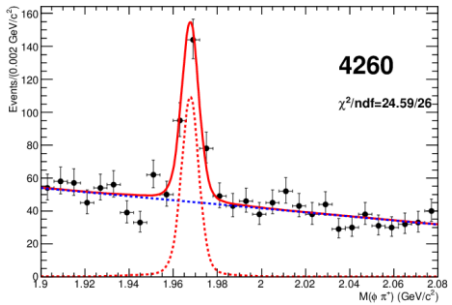

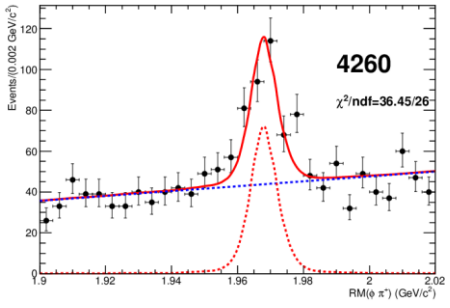

Goodness of 2D fit

The χ^2/ndf for most data is around 1,
For 4009 data, a little high.

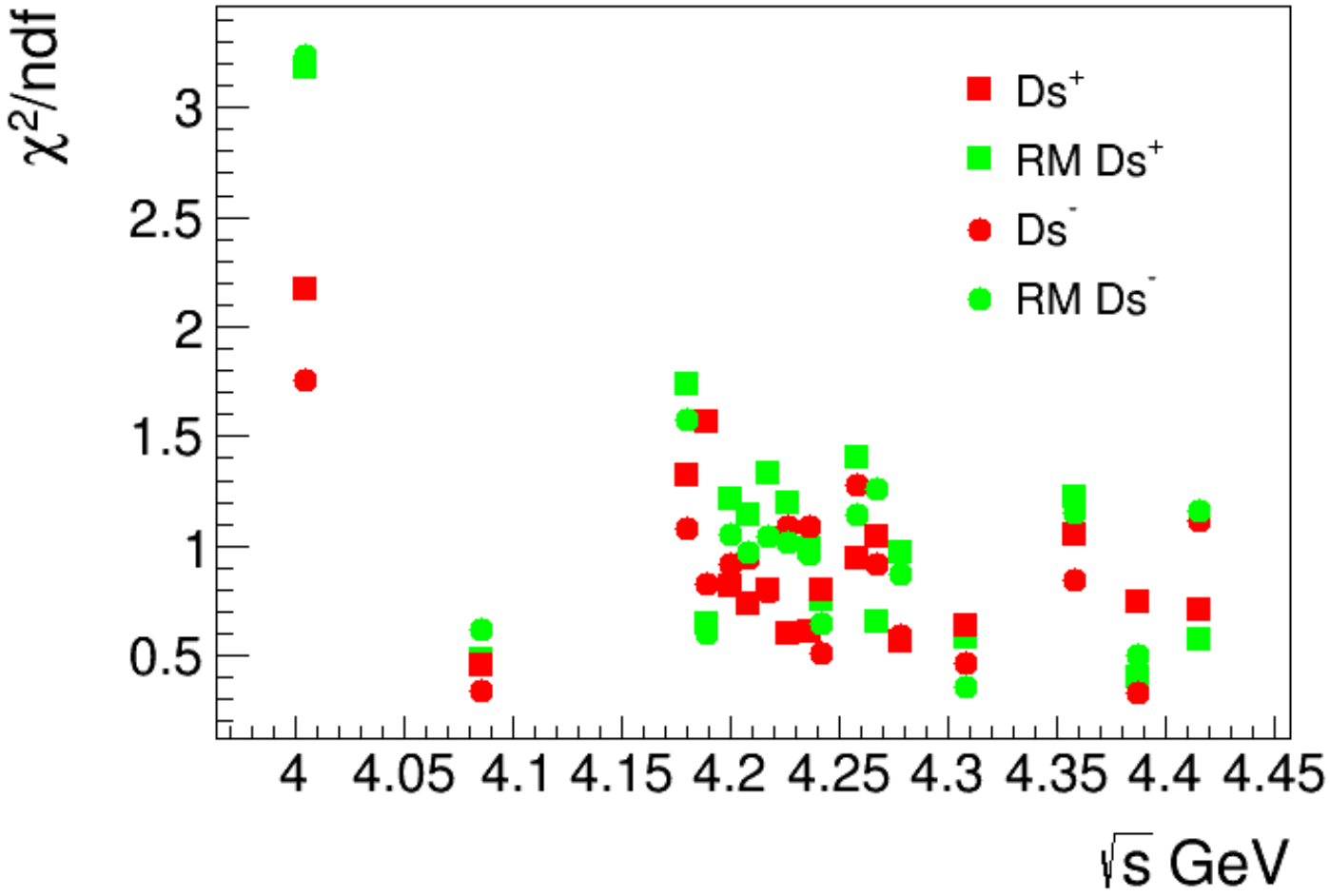

Rscan data

- 2D sideband substraction of R-scan data crashed since the estimated number of backgrounds in signal region (red box):

$n_{red} = \frac{n_{blue}}{2} + \frac{n_{green}}{2} - \frac{n_{black}}{4}$ could be negative.

- Use 1D sideband for R-scan data since no non-D_s^+ real-D_s^- is observed.

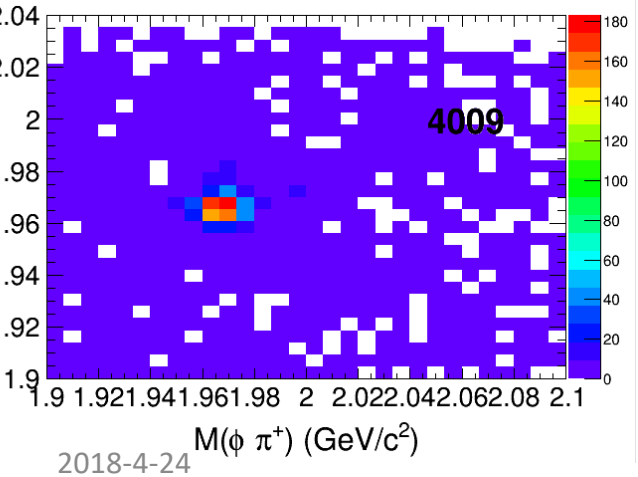

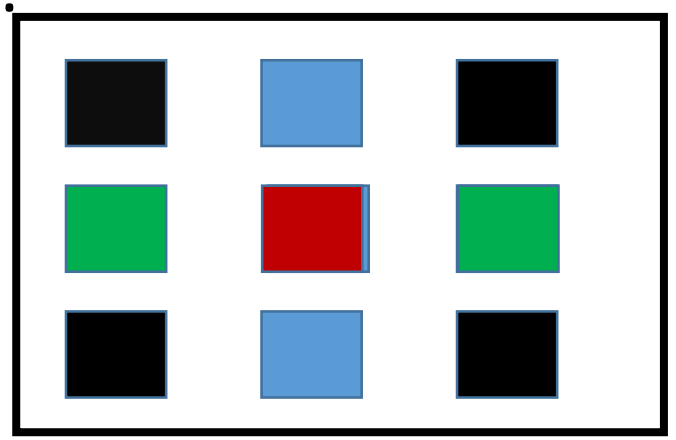

Cross sections

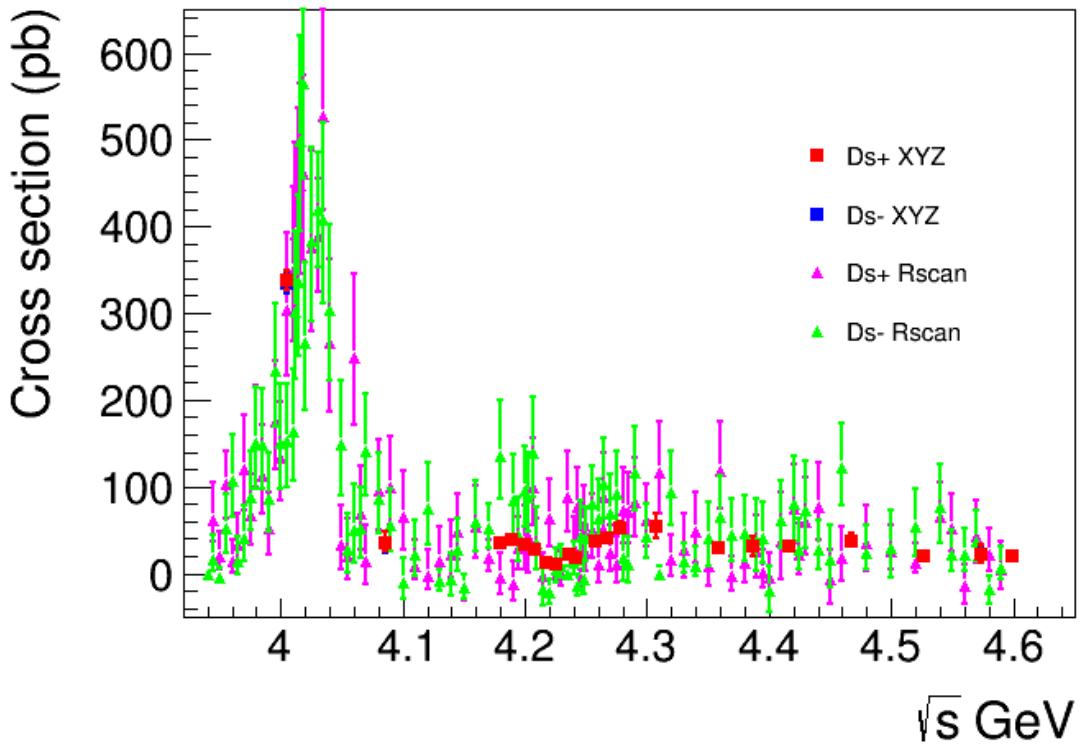

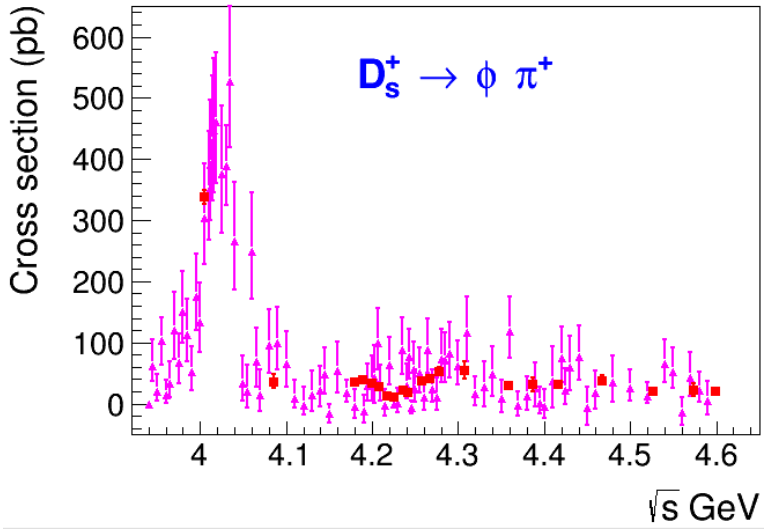

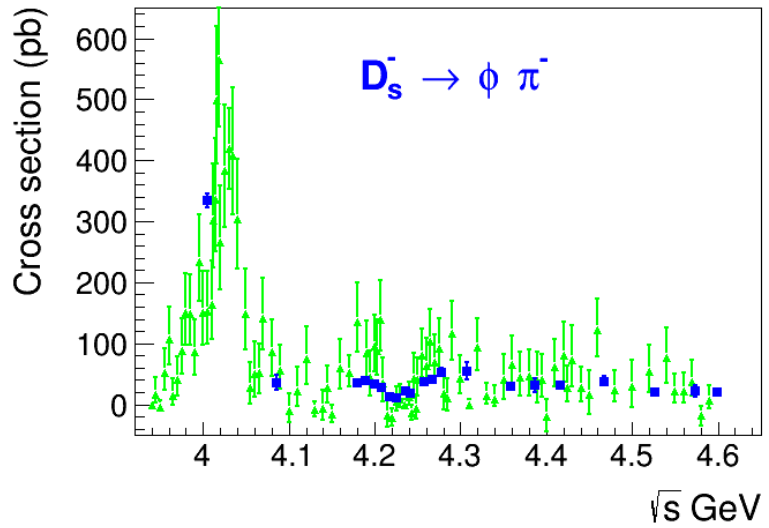

After ISR and vacuum polarization corrections.
Good consistence between D_s^+ andD_s^- tag , and XYZ and R-scan results.

Combine the D_s^+ and D_s^-

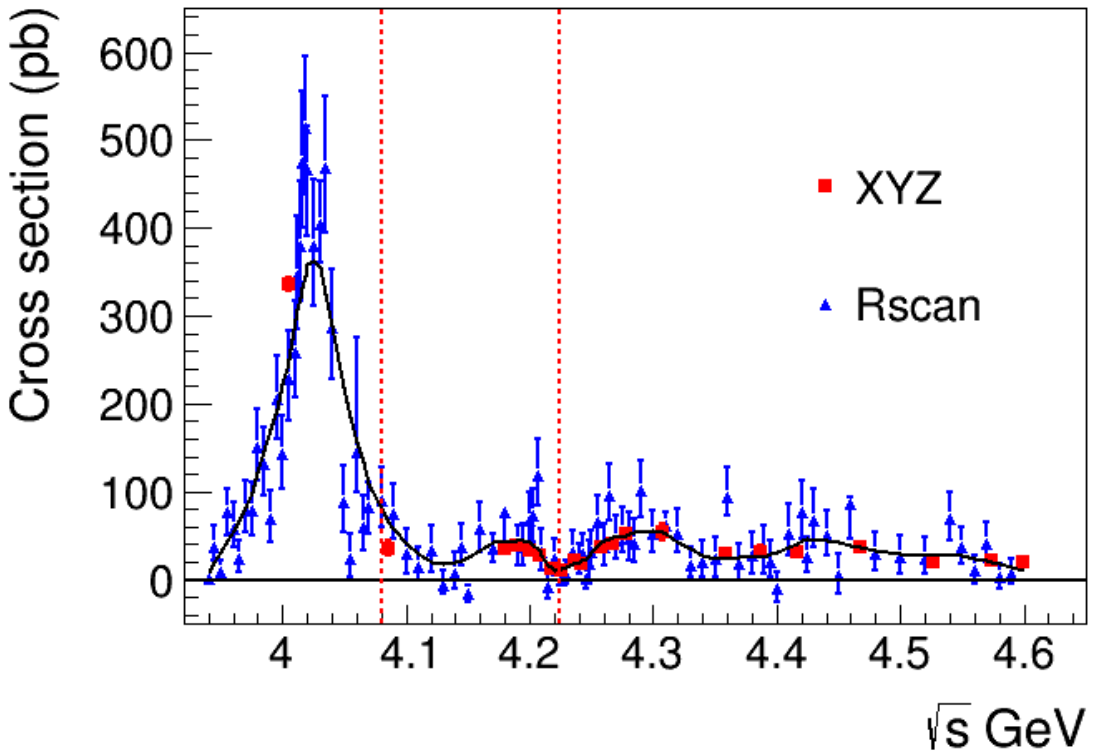

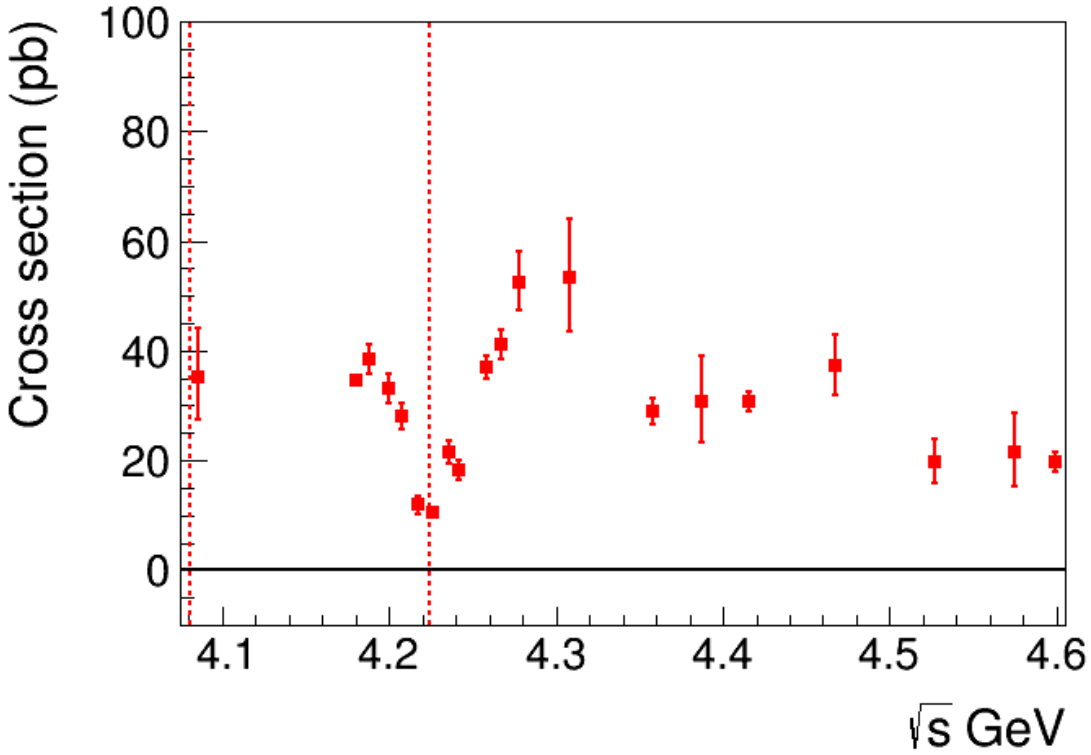

Difficult to parameterize the lineshape, so use a smooth method (LOWESS) .

Red dashed lines show the threshold of $D_s^* D_s$ and $D_s^* D_s^*$

Numbers with stat. and syst. uncertainties.

4004	$336.1^{+8.2}_{-8.1} \pm 26.9$	4085	$35.3^{+9.0}_{-7.9} \pm 2.9$
4180	$34.7^{+1.1}_{-1.1} \pm 2.8$	4189	$38.5^{+2.8}_{-2.7} \pm 3.1$
4200	$33.1^{+2.7}_{-2.6} \pm 2.8$	4208	$28.1^{+2.4}_{-2.3} \pm 2.3$
4217	$11.9^{+1.7}_{-1.6} \pm 1.0$	4226	$10.6^{+1.2}_{-1.1} \pm 0.9$
4236	$21.4^{+2.2}_{-2.1} \pm 1.7$	4242	$18.2^{+2.0}_{-1.9} \pm 1.5$
4258	$36.8^{+2.2}_{-2.1} \pm 3.0$	4267	$41.1^{+2.8}_{-2.7} \pm 3.3$
4278	$52.6^{+5.5}_{-5.1} \pm 4.2$	4308	$53.3^{+10.8}_{-9.6} \pm 4.3$
4358	$28.9^{+2.4}_{-2.3} \pm 2.4$	4387	$30.7^{+8.4}_{-7.4} \pm 2.5$
4416	$30.7^{+1.7}_{-1.7} \pm 2.5$	4467	$37.3^{+5.7}_{-5.3} \pm 3.0$
4527	$19.7^{+4.3}_{-3.9} \pm 1.6$	4574	$21.4^{+7.2}_{-6.1} \pm 1.7$
4600	$19.6^{+1.9}_{-1.8} \pm 1.6$		

3950	$8.4^{+12.7}_{-7.1} \pm 0.7$	3955	$76.9^{+26.5}_{-27.0} \pm 6.2$	3960	$58.5^{+28.7}_{-22.5} \pm 4.7$
3965	$23.2^{+21.6}_{-14.9} \pm 1.9$	3970	$78.1^{+35.3}_{-25.0} \pm 6.3$	3975	$77.8^{+33.6}_{-27.0} \pm 6.2$
3980	$150.2^{+44.8}_{-38.0} \pm 12.1$	3985	$130.9^{+41.9}_{-35.2} \pm 10.5$	3990	$68.8^{+32.5}_{-25.8} \pm 5.5$
3995	$204.7^{+50.9}_{-44.0} \pm 16.4$	4000	$142.0^{+45.0}_{-38.0} \pm 11.4$	4005	$227.9^{+54.3}_{-47.4} \pm 18.5$
4010	$258.6^{+58.7}_{-51.6} \pm 21.0$	4012	$345.5^{+68.4}_{-60.9} \pm 28.0$	4014	$379.8^{+73.7}_{-62.7} \pm 30.8$
4016	$474.0^{+82.4}_{-74.1} \pm 38.0$	4018	$513.1^{+83.0}_{-75.2} \pm 41.1$	4020	$466.0^{+49.2}_{-75.6} \pm 37.4$
4025	$379.3^{+76.2}_{-67.8} \pm 30.6$	4030	$405.0^{+48.0}_{-44.7} \pm 32.7$	4035	$468.0^{+82.1}_{-74.0} \pm 37.7$
4040	$286.2^{+67.1}_{-58.8} \pm 23.0$	4050	$87.9^{+42.4}_{-34.4} \pm 7.1$	4055	$24.0^{+28.1}_{-20.5} \pm 1.9$
4060	$144.7^{+131.5}_{-45.1} \pm 11.7$	4065	$59.8^{+35.1}_{-27.5} \pm 4.8$	4070	$83.0^{+28.3}_{-30.8} \pm 6.7$
4080	$90.1^{+38.1}_{-31.4} \pm 7.2$	4090	$74.0^{+35.0}_{-27.2} \pm 6.0$	4100	$28.9^{+28.7}_{-22.2} \pm 2.4$
4110	$14.5^{+23.2}_{-15.8} \pm 1.2$	4120	$32.3^{+30.0}_{-23.7} \pm 2.6$	4130	$-5.8^{+16.9}_{-9.6} \pm 0.5$
4140	$7.4^{+23.5}_{-16.9} \pm 0.6$	4145	$36.8^{+27.2}_{-20.5} \pm 2.9$	4150	$-16.5^{+9.7}_{-9.3} \pm 1.3$
4160	$56.9^{+32.1}_{-25.7} \pm 4.6$	4170	$34.5^{+17.1}_{-14.4} \pm 2.8$	4180	$77.0^{+3.0}_{-36.9} \pm 6.2$
4190	$40.0^{+21.1}_{-23.1} \pm 3.2$	4195	$36.2^{+26.7}_{-20.1} \pm 2.9$	4200	$67.1^{+32.5}_{-25.7} \pm 5.6$
4203	$72.0^{+31.3}_{-29.7} \pm 6.0$	4206	$119.0^{+41.6}_{-35.1} \pm 9.5$	4210	$30.9^{+26.1}_{-19.6} \pm 2.5$
4215	$-7.8^{+17.0}_{-13.3} \pm 0.6$	4220	$22.8^{+23.0}_{-18.1} \pm 1.8$	4225	$-0.5^{+9.6}_{-4.9} \pm 0.0$
4230	$4.9^{+16.0}_{-10.1} \pm 0.4$	4235	$31.4^{+24.3}_{--24.3} \pm 2.5$	4240	$20.7^{+20.1}_{-14.0} \pm 1.7$
4243	$29.0^{+23.6}_{-11.1} \pm 2.3$	4245	$1.0^{+23.3}_{-10.9} \pm 0.1$	4248	$18.3^{+25.9}_{-20.7} \pm 1.5$
4250	$32.2^{+23.0}_{-17.4} \pm 2.6$	4255	$65.2^{+29.6}_{-23.6} \pm 5.2$	4260	$37.6^{+26.0}_{-20.9} \pm 3.0$
4265	$96.5^{+34.9}_{-29.2} \pm 7.8$	4270	$45.4^{+26.7}_{-21.2} \pm 3.6$	4275	$54.0^{+28.4}_{-23.0} \pm 4.3$
4280	$45.9^{+29.9}_{-24.7} \pm 3.7$	4285	$41.4^{+27.1}_{-21.7} \pm 3.3$	4290	$100.5^{+35.6}_{-30.3} \pm 8.1$
4300	$52.8^{+26.4}_{-20.9} \pm 4.3$	4310	$61.6^{+14.2}_{--13.9} \pm 5.0$	4320	$52.9^{+27.0}_{-22.3} \pm 4.3$
4330	$16.9^{+20.1}_{-13.6} \pm 1.4$	4340	$20.1^{+23.7}_{-16.9} \pm 1.6$	4350	$23.3^{+25.1}_{-20.0} \pm 1.9$
4360	$93.4^{+35.4}_{-20.7} \pm 7.6$	4370	$17.6^{+23.5}_{-18.6} \pm 1.4$	4380	$28.1^{+26.0}_{-20.7} \pm 2.3$
4390	$31.4^{+30.3}_{-24.6} \pm 2.6$	4395	$20.6^{+23.6}_{-17.9} \pm 1.7$	4400	$-10.3^{+18.1}_{-15.6} \pm 0.8$
4410	$53.0^{+33.1}_{-25.3} \pm 4.2$	4420	$76.7^{+36.4}_{-30.4} \pm 6.1$	4425	$25.6^{+23.2}_{-17.1} \pm 2.1$
4430	$66.4^{+36.8}_{-30.2} \pm 5.3$	4440	$49.6^{+29.1}_{-23.1} \pm 4.0$	4450	$4.3^{+25.9}_{-21.2} \pm 0.3$
4460	$85.9^{+7.6}_{-39.0} \pm 6.9$	4480	$28.4^{+24.8}_{-18.7} \pm 2.3$	4500	$26.1^{+24.8}_{-18.7} \pm 2.1$
4520	$23.7^{+24.1}_{-16.2} \pm 1.9$	4540	$69.2^{+30.5}_{-25.3} \pm 5.6$	4550	$36.9^{+22.9}_{-18.0} \pm 3.0$
4560	$9.8^{+18.0}_{-13.6} \pm 0.8$	4570	$40.4^{+25.7}_{-20.3} \pm 3.3$	4580	$3.1^{+15.7}_{-14.4} \pm 0.3$
4590	$6.5^{+17.6}_{-11.6} \pm 0.5$	3940	$0.4^{+5.5}_{-1.0} \pm 0.0$	3945	$36.4^{+25.8}_{-14.3} \pm 2.9$

Systematic uncertainty

- Simple event selections.
- Tracking and PID, 1% for each track.
- Branching fraction of $D_s \to \phi\pi \to K^+K^-\pi$, 4.5% from PDG
- Fit range: change 1 standard deviation, less than
  2% difference in number of signal events
- Background shape: alter the shape from 1-order to
  2-order polynomial, around 2%

use 4009 and
4180 data,
Largest statistics

Systematic uncertainty

ISR correction:

Take the difference between last two iteration as systematic uncertainty.

Around 1%.

Total systematic uncertainty: around 8%.

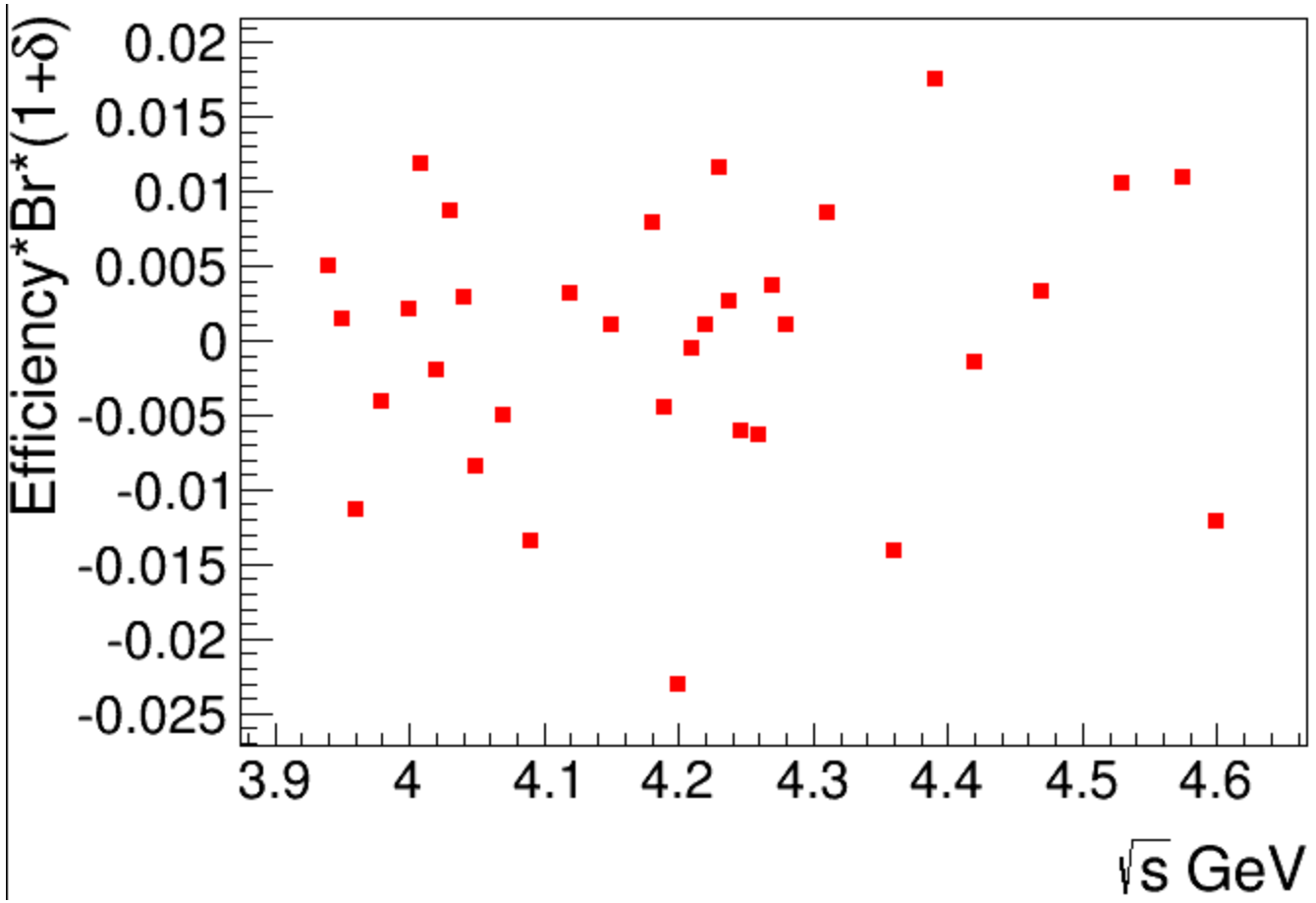

Summary

- Update the analysis of $e^+e^- \to D_s^+ D_s^-$ with ConExc and 2D fit.
- Results are consist well between D_s^+ and D_s^- tags, XYZ and R-scan data.
- Updating the memo accordingly now. Release it in this week.

Thanks for your attention.

Back-up

- Following are the slides for previous talk.

Introduction

- We all know $Y(4260)$ but we all do not know its nature.
- Above open-charm threshold, all the vector charmonium are expected to decay dominantly to open-charm channels.
- Coupling between Y and open-charm channels are different in different theoretical models.
- Previous results from BaBar, Belle and CLEOc have bad precision.
- At BESIII, we can do better.

Data sets and MC simulation

- All the data above the threshold of $D_s^+ D_s^-$, including R-scan data.

ID	$\sqrt{s}$ (MeV)	Luminosity(pb^{-1})
4008	4007.62	481.96
4085	4085.45	52.63
4189	4188.59	43.09
4208	4207.73	54.55
4217	4217.12	54.13
4226	4226.26	1047.34
4242	4241.66	55.59
4258	4257.97	825.67
4308	4307.89	44.90
4358	4358.26	539.84
4387	4387.40	55.18
4416	4415.58	1073.56
4467	4467.06	109.94
4527	4527.14	109.98
4575	4574.50	47.67
4600	4599.53	566.93
4180	4180	3189.0
4190	4189.3	521.9
4200	4199.6	523.7
4210	4209.7	511.2
4220	4218.8	508.2
4237	4235.8	508.9
4246	4243.9	532.7
4270	4266.9	529.3
4280	4277.8	174.5

New data.

Data sets and MC simulation

- BOSS version: 703
- Decay model in EvtGen:
  - $e^+e^- \to D_s^+ D_s^-$: VSS
  - $D_s \to K^+K^-\pi$: result from Dalitz analysis
- Two sets of exclusive MC,
  - $D_s^+ \to K^+K^-\pi^+, D_s^- \to X$
  - $D_s^- \to K^+K^-\pi^-, D_s^+ \to X$
- 34 energy points

Each of them contains 50,000 events.

3940	4009	4050	4110	4230	4360	4500
3950	4014	4060	4130	4260	4390	4530
3960	4020	4070	4150	4285	4420	4570
3980	4030	4080	4170	4310	4440	4600
4000	4040	4090	4190	4340	4470	

Analysis strategy

- Only reconstruct one D_s with $\phi\pi$
- Set requirement on the recoil mass distribution
- Extract signal yield using invariant mass of $\phi\pi$
- Combine the results of D_s^+ and D_s^-
- Overlap is about 0.5% percent, so the corresponding effect on statistical error could be neglected.

Event selections

- At least three good charged tracks with $|V_z| < 10$ and

$$\sqrt{V_x^2 + V_y^2} < 1 \text{ cm}$$

- PID to identify kaon and pion
- Keep all the combinations
- Mass window of ϕ : [1.005, 1.034] GeV ([$\pm$1.5FWHM])

Invariant mass of K^+K^-

- Double Gaussian plus Argus.

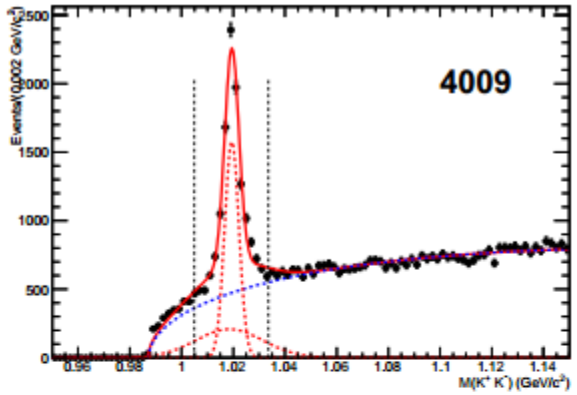

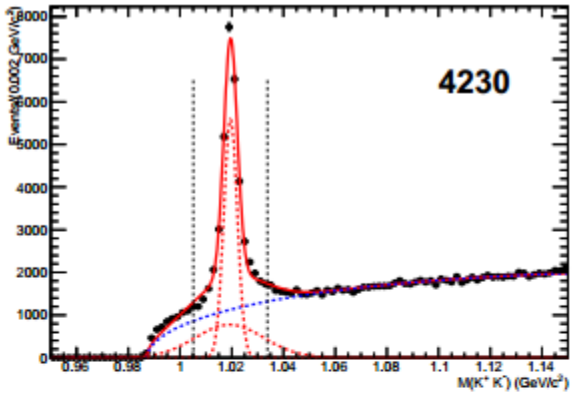

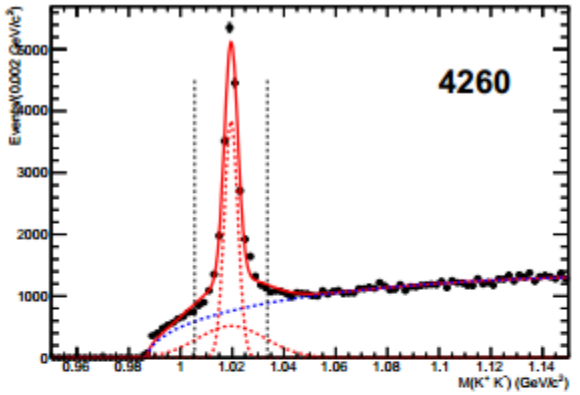

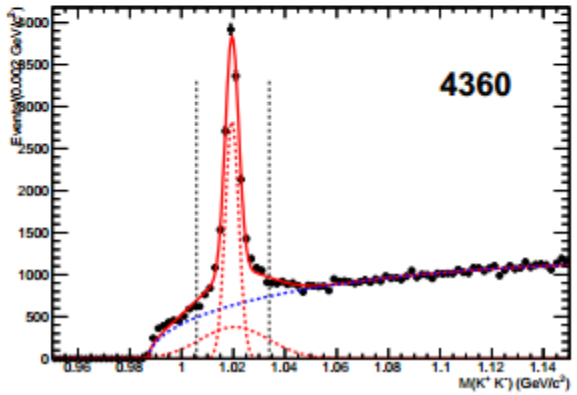

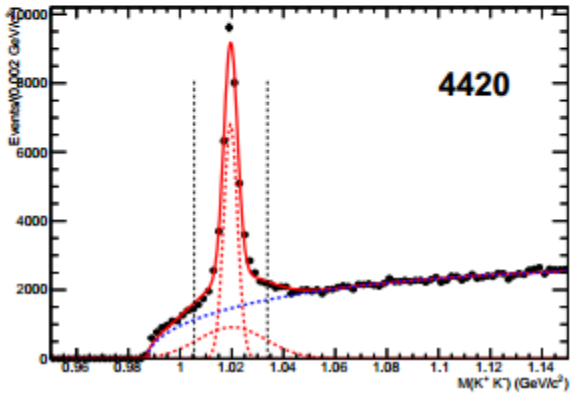

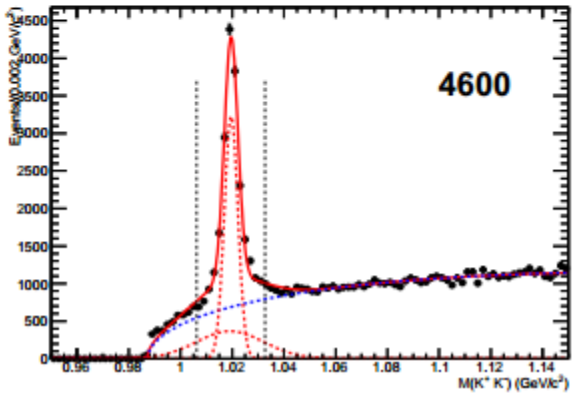

Invariant mass of $\phi\pi$

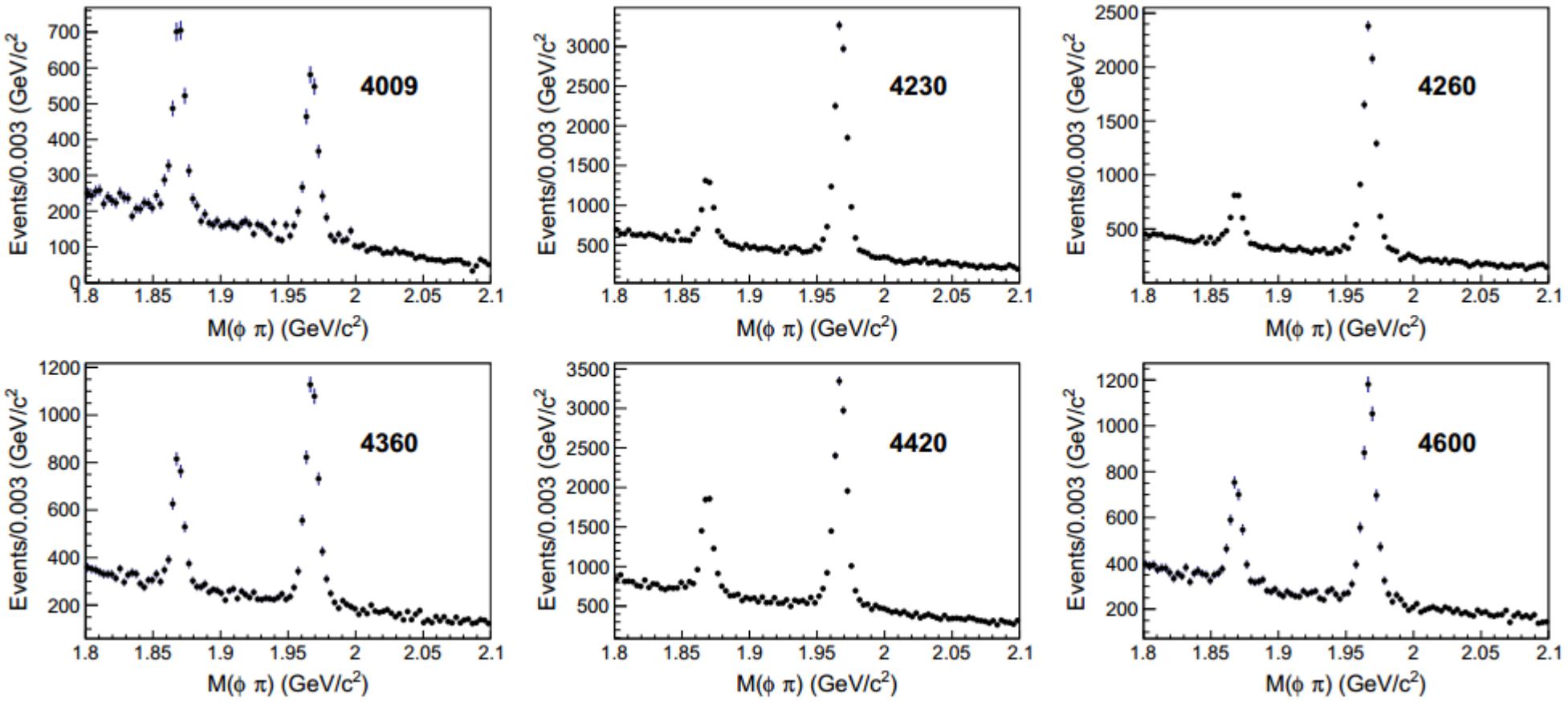

Two peaks, first one is $D^{\pm}$, second one is $D_s^{\pm}$

Recoil mass of $\phi\pi$

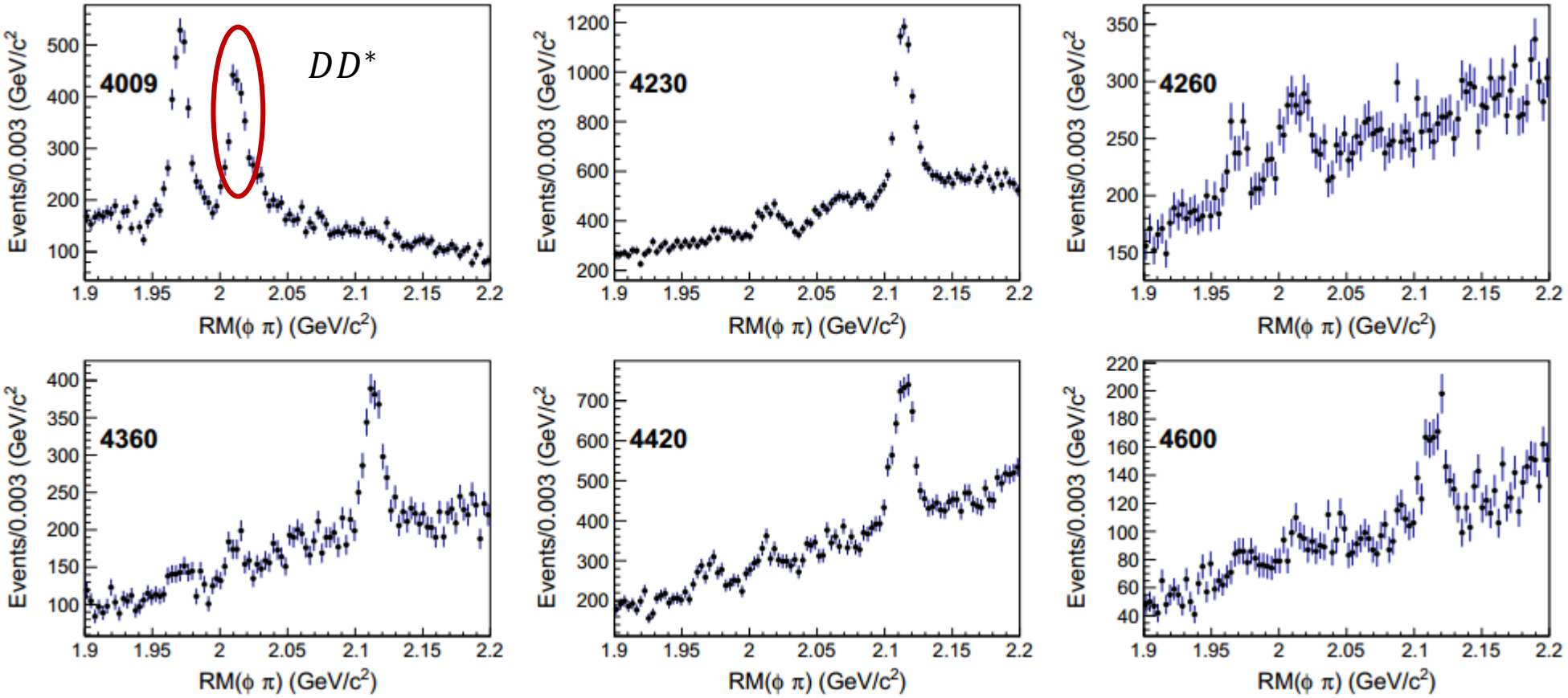

Background from DD^*, but can be separately well in $M(\phi\pi)$

$D_s^* D_s^*$ is far away from signal peak.

Mass resolution

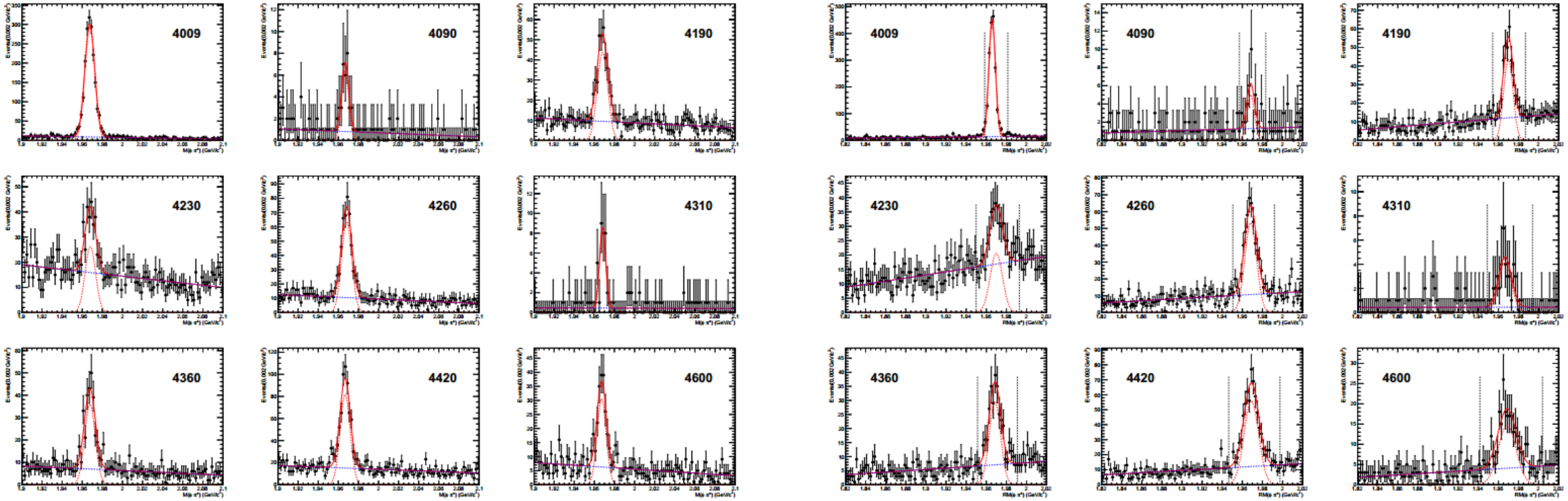

Invariant mass of $\phi\pi$ recoil mass of $\phi\pi$

Single Gaussian and a linear background.

Resolutions of for the reconstructed D_s are almost the same,

but the resolution for the missing D_s increase along c.m. energy.

Mass resolution

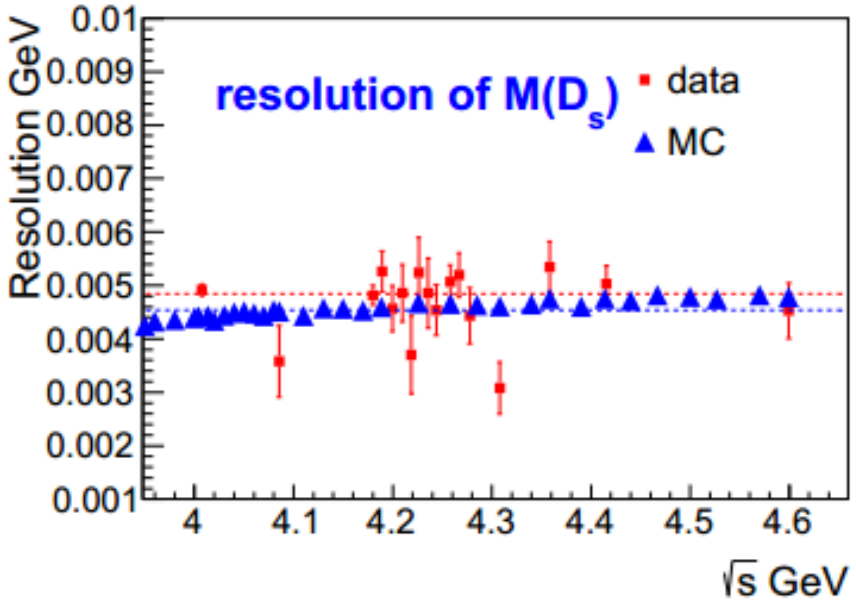

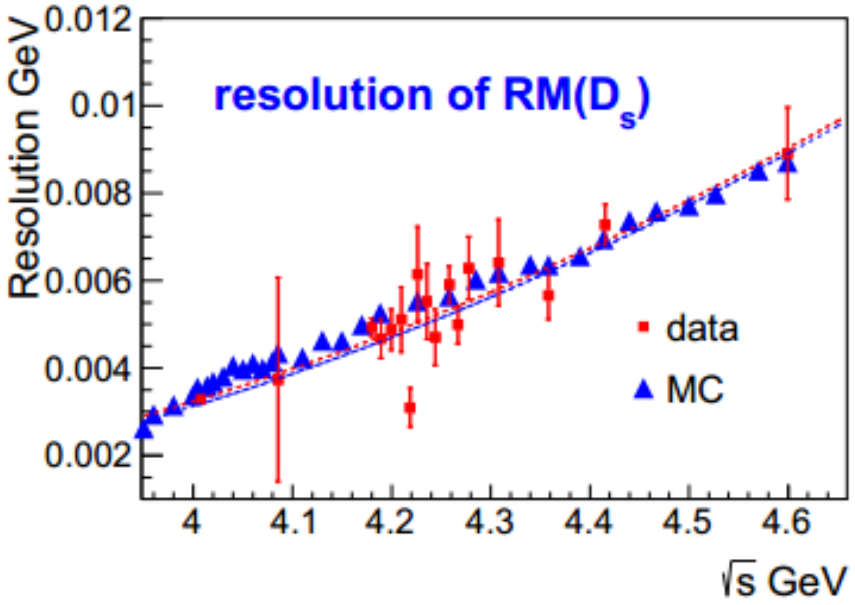

- Resolution from data and MC simulation agree well.
- Set mass window for the missing D_s as $[\mu - 3 \cdot \sigma, \mu + 4 \cdot \sigma]$ to include the ISR events
- Fit the invariant mass of $\phi\pi$, and fix the shape.

Extract signal yield

- XYZ data:
  - Signal shape: Gaussian
  - Background: linear
- XYZ scan data:
  - Fix the parameter of backgr

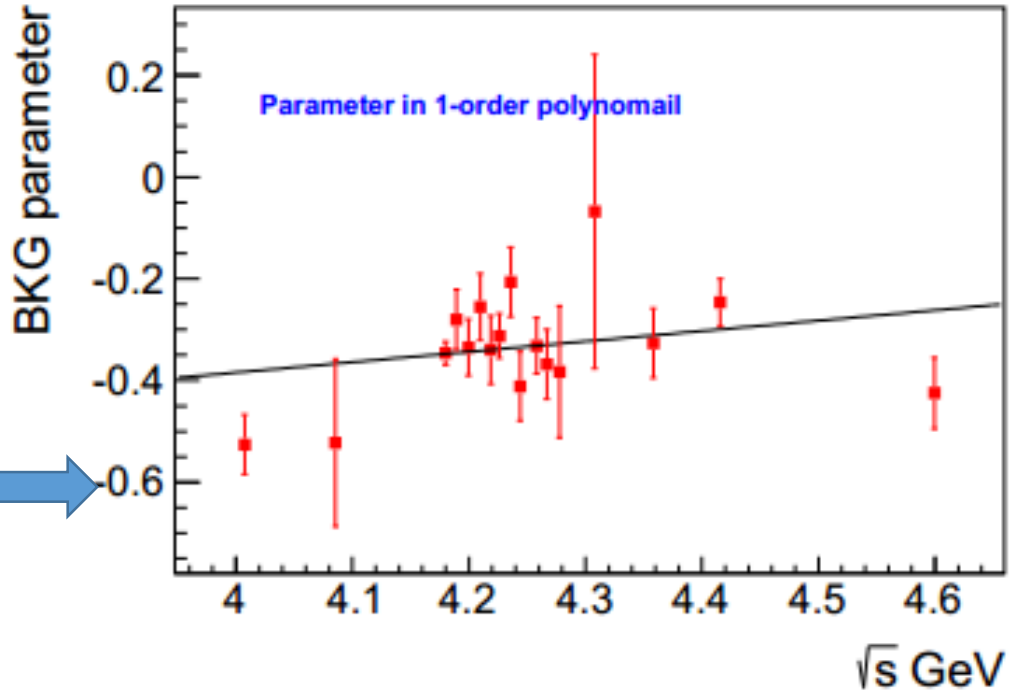

Extract signal yield

- R-scan data:
  - Statistics is not enough for fit.
  - Count the numbers of events in signal ($[\mu - 3 \cdot \sigma, \mu + 3 \cdot \sigma]$) and sideband regions (outside $[\mu - 4 \cdot \sigma, \mu + 4 \cdot \sigma]$) as n and b
  - Assuming they follow Poisson distributions
  - Define likelihood:

$$L(s) = L(n - b \cdot f) = \int P(n; x) \cdot P(b; \frac{s - x}{f}) dx,$$

  - Statistical error
    - $\ln(L(s - \sigma^-)) = \ln(L(s + \sigma^+)) = \ln\big(L(s)\big) - 0.5$

Observed cross sections

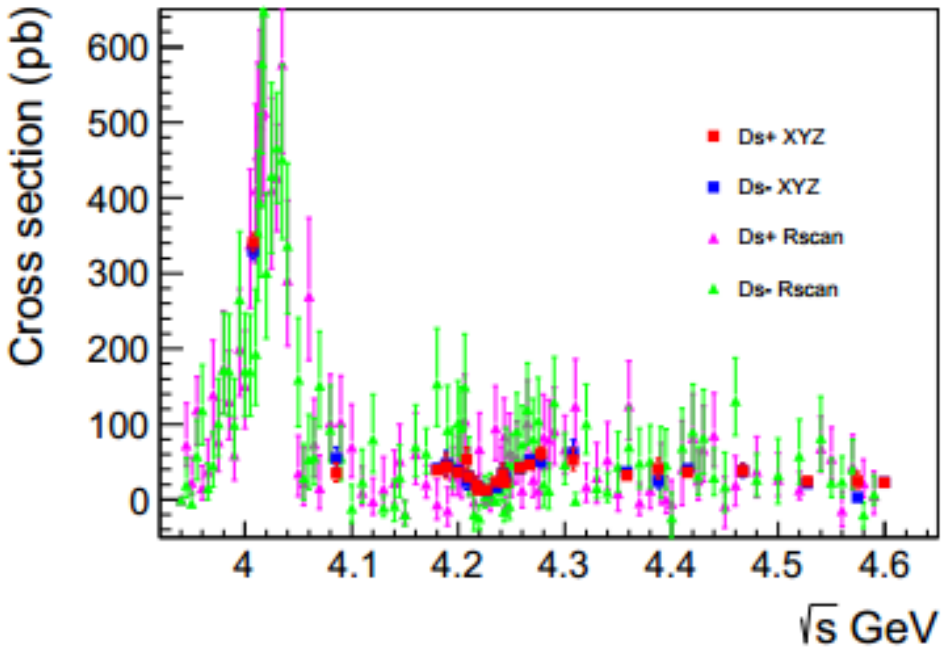

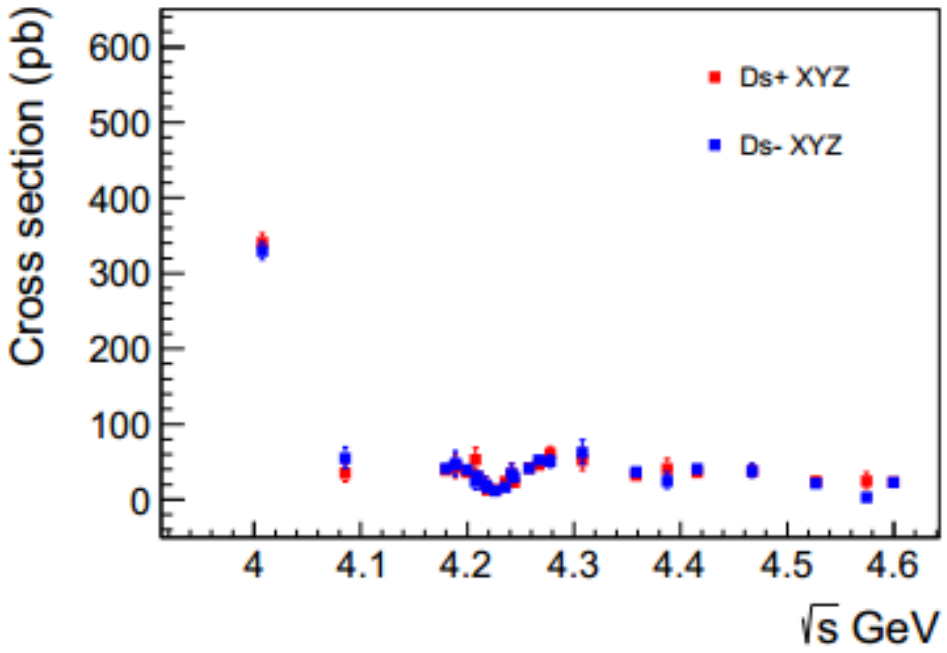

- Results from XYZ and R-scan data consist with each other.
- Results from tagged D_s^+ and D_s^- consist with each other.
- Clear peak of $\psi(4040)$.
- Dip around 4.22 GeV.

Born cross sections

$$\sigma^B = \frac{\sigma^{\rm obs}}{(1+\delta)(1+\delta^{\rm vac})} = \frac{n^{\rm obs}}{\mathcal{L}\mathcal{B}\epsilon(1+\delta)(1+\delta^{vac})},$$

- Vacuum polarization correction factor $(1+\delta^{vac})$is only dependent with c.m. energy
- ISR correction $(1+\delta)$ is obtained by iteration.
- Cross section are parameterized using a smooth method, LOWESS

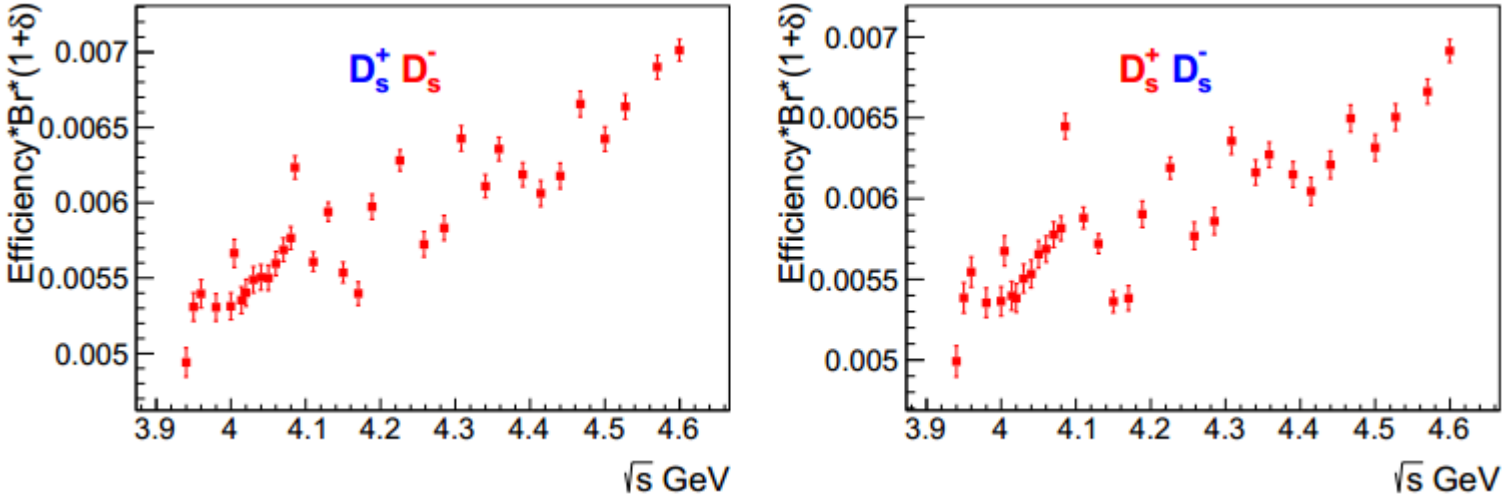

Born cross sections

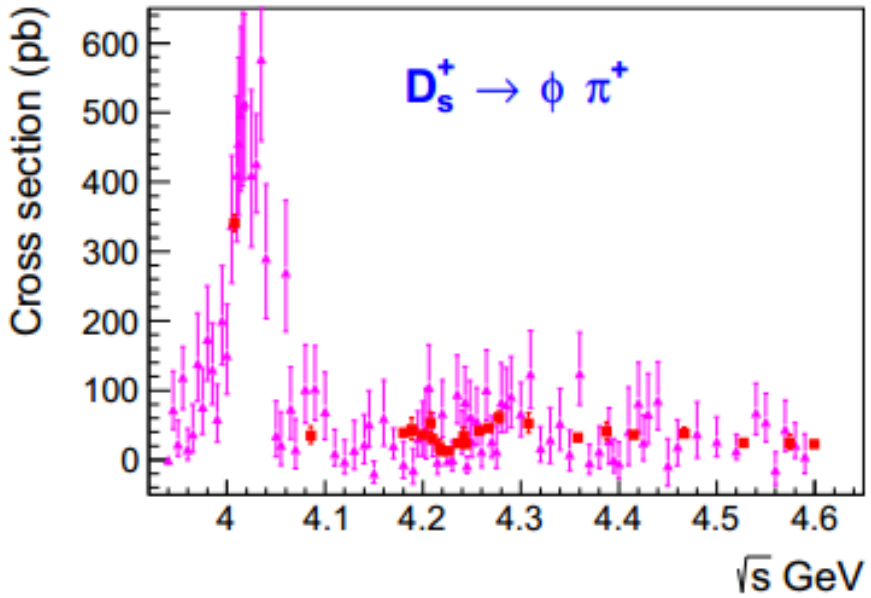

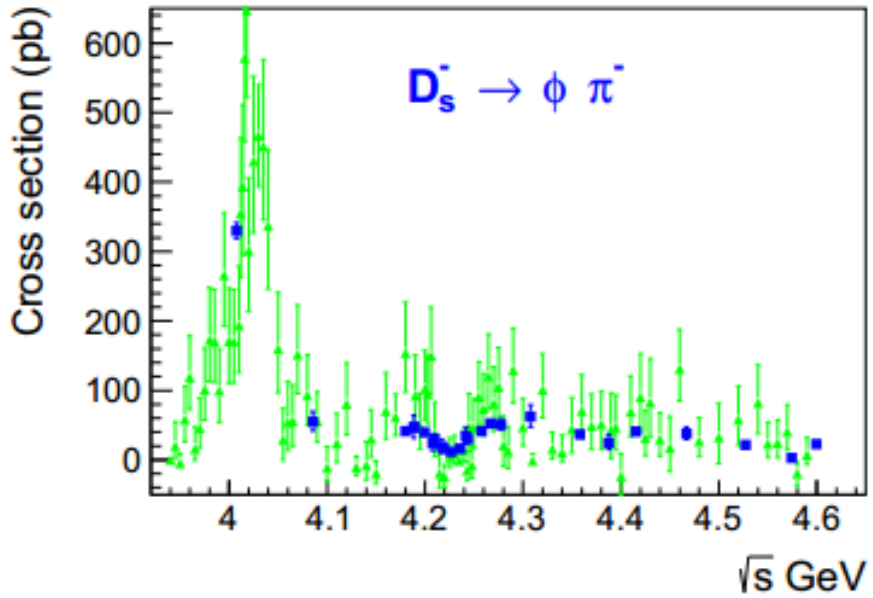

Combine the results of tagged D_s^+ and D_s^-.
The combined likelihood:

$$L(\sigma_0) = \int\int L_1(\sigma_1)\cdot L_2(\sigma_2)\,|_{\sigma_1=\sigma_2=\sigma_0} = L_1(\sigma_0)\cdot L_2(\sigma_0).$$

Born cross sections

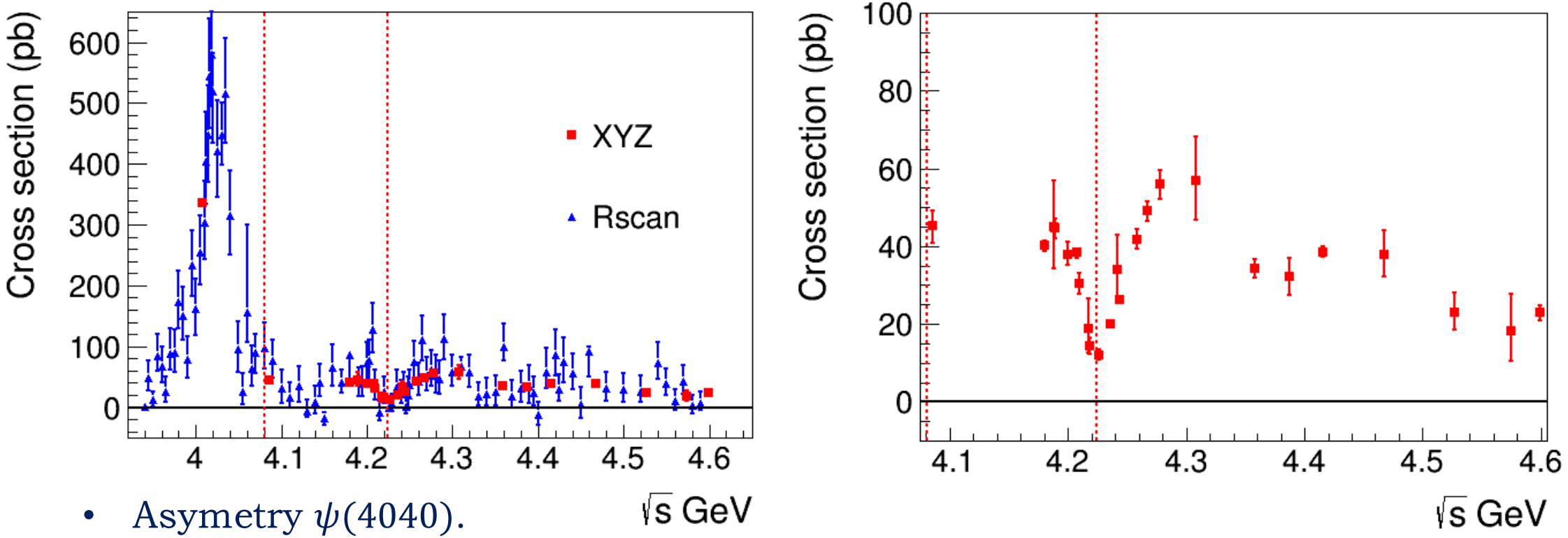

- Asymetry $\psi(4040)$.
- Dip at 4.22 GeV, just at the threshold of $D_s^* D_s^*$
- Cross section goes down at 4.31 GeV then goes up at 4.42 GeV.
- The dip could be caused by interference between Y(4260), $\psi(4160)$ and other states, or the threshold effect of $D_s^* D_s^*$. Unlike the $f_0(980)$, the cross section decrease below the threshold of $D_s^* D_s^*$ and has minimum value at the threshold.

Born cross sections

- Numbers are listed here

$\sqrt{s}$ (MeV)	σ^B (pb)	$\sqrt{s}$ (MeV)	σ^B (pb)
4008	$335.3^{+7.0}_{-7.0} \pm 2.2$	4085	$45.4^{+3.8}_{-4.5} \pm 0.0$
4189	$45.0^{+12.0}_{-10.7} \pm 1.5$	4208	$38.4^{+-1.3}_{-1.3} \pm 2.6$
4217	$18.9^{+7.5}_{-6.5} \pm 1.6$	4226	$12.1^{+1.4}_{-1.3} \pm 1.2$
4242	$34.0^{+9.0}_{-8.0} \pm 3.0$	4258	$41.8^{+2.5}_{-2.4} \pm 3.2$
4308	$57.0^{+11.2}_{-10.1} \pm 6.9$	4358	$34.2^{+2.3}_{-2.3} \pm 0.3$
4387	$32.3^{+4.8}_{-4.7} \pm 0.4$	4416	$38.6^{+1.4}_{-1.4} \pm 1.9$
4467	$38.0^{+6.1}_{-5.7} \pm 1.1$	4527	$23.1^{+4.9}_{-4.5} \pm 1.0$
4574	$18.3^{+9.3}_{-7.7} \pm 0.6$	4600	$22.9^{+2.1}_{-2.0} \pm 0.7$
4180	$40.1^{+1.3}_{-1.3} \pm 0.3$	4189	$44.6^{+2.7}_{-2.6} \pm 1.6$
4200	$38.0^{+3.1}_{-3.0} \pm 2.0$	4210	$30.5^{+2.8}_{-2.6} \pm 2.2$
4129	$14.4^{+2.1}_{-2.0} \pm 0.9$	4236	$20.2^{+0.4}_{-0.6} \pm 1.9$
4244	$26.2^{+1.0}_{-1.1} \pm 2.3$	4267	$49.1^{+2.6}_{-2.5} \pm 1.5$
4278	$56.0^{+3.7}_{-3.8} \pm 1.3$		

$\sqrt{s}$ (MeV)	σ^B (pb)	$\sqrt{s}$ (MeV)	σ^B (pb)		
3940	$0.2^{+5.7}_{-0.9} \pm 0.0$	3945	$47.4^{+29.7}_{-20.4} \pm 2.0$	3950	$11.5^{+14.1}_{-10.1} \pm 0.3$
3955	$85.1^{+35.1}_{-25.6} \pm 2.3$	3960	$66.3^{+32.4}_{-25.4} \pm 1.9$	3965	$26.2^{+24.6}_{-16.8} \pm 0.8$
3970	$88.8^{+40.7}_{-27.6} \pm 2.6$	3975	$89.4^{+38.6}_{-31.1} \pm 2.6$	3980	$173.5^{+51.8}_{-43.9} \pm 5.0$
3985	$150.4^{+48.2}_{-40.5} \pm 3.9$	3990	$78.7^{+37.2}_{-29.5} \pm 1.8$	3995	$233.2^{+57.9}_{-50.1} \pm 4.8$
4000	$161.0^{+51.0}_{-43.1} \pm 2.9$	4005	$254.4^{+60.7}_{-52.9} \pm 5.4$	4010	$303.9^{+68.9}_{-60.6} \pm 2.1$
4012	$404.9^{+80.1}_{-71.3} \pm 7.4$	4014	$448.1^{+82.1}_{-78.2} \pm 13.5$	4016	$544.9^{+94.8}_{-85.2} \pm 30.0$
4018	$580.6^{+93.9}_{-85.1} \pm 46.4$	4020	$519.5^{+62.4}_{-84.2} \pm 54.4$	4025	$420.6^{+84.5}_{-75.2} \pm 49.9$
4030	$447.0^{+52.9}_{-49.3} \pm 59.2$	4035	$515.6^{+90.5}_{-81.5} \pm 65.3$	4040	$314.8^{+73.8}_{-64.7} \pm 38.0$
4050	$95.4^{+46.0}_{-37.3} \pm 8.9$	4055	$26.0^{+30.4}_{-22.1} \pm 2.0$	4060	$156.4^{+143.7}_{-48.8} \pm 9.8$
4065	$64.4^{+37.7}_{-29.6} \pm 3.8$	4070	$89.1^{+30.4}_{-33.1} \pm 5.0$	4080	$97.4^{+41.2}_{-33.9} \pm 3.1$
4090	$76.4^{+35.0}_{-28.7} \pm 0.6$	4100	$30.4^{+30.4}_{-23.5} \pm 0.7$	4110	$16.0^{+25.4}_{-17.4} \pm 0.6$
4120	$34.6^{+32.4}_{-25.6} \pm 1.0$	4130	$-6.1^{+18.5}_{-10.4} \pm 0.1$	4140	$8.5^{+25.8}_{-18.5} \pm 0.2$
4145	$41.1^{+30.2}_{-22.8} \pm 1.4$	4150	$-18.6^{+11.0}_{-10.5} \pm 0.8$	4160	$65.6^{+37.0}_{-29.6} \pm 2.9$
4170	$40.6^{+20.1}_{-16.9} \pm 1.9$	4180	$86.9^{+3.4}_{-41.5} \pm 0.2$	4190	$43.4^{+22.6}_{-25.2} \pm 1.6$
4195	$39.2^{+28.9}_{-21.8} \pm 1.8$	4200	$72.5^{+34.5}_{-28.1} \pm 4.0$	4203	$75.9^{+35.2}_{-30.8} \pm 4.6$
4206	$127.2^{+44.5}_{-37.6} \pm 8.3$	4210	$32.8^{+27.8}_{-20.9} \pm 2.4$	4215	$-8.1^{+18.2}_{-14.1} \pm 0.7$
4220	$25.0^{+24.7}_{-19.3} \pm 2.3$	4225	$-0.6^{+10.1}_{-5.1} \pm 0.1$	4230	$5.2^{+17.2}_{-10.9} \pm 0.5$
4235	$33.7^{+27.3}_{--27.3} \pm 3.2$	4240	$22.6^{+22.3}_{-15.2} \pm 2.0$	4243	$32.4^{+26.1}_{-12.7} \pm 2.9$
4245	$0.8^{+26.1}_{-11.8} \pm 0.1$	4248	$20.7^{+29.0}_{-23.2} \pm 1.7$	4250	$36.2^{+25.9}_{-19.6} \pm 3.0$
4255	$74.6^{+33.5}_{-27.1} \pm 5.9$	4260	$42.9^{+29.8}_{-23.9} \pm 2.7$	4265	$110.8^{+40.0}_{-33.6} \pm 3.0$
4270	$52.1^{+30.8}_{-24.4} \pm 0.4$	4275	$61.5^{+32.4}_{-26.2} \pm 2.7$	4280	$51.6^{+33.7}_{-27.9} \pm 4.0$
4285	$46.8^{+30.6}_{-24.6} \pm 5.3$	4290	$112.1^{+39.7}_{-33.8} \pm 12.9$	4300	$57.1^{+28.9}_{-22.5} \pm 6.8$
4310	$66.5^{+15.1}_{--13.5} \pm 7.7$	4320	$57.1^{+29.2}_{-24.1} \pm 5.2$	4330	$18.8^{+21.4}_{-15.2} \pm 1.2$
4340	$22.3^{+26.2}_{-18.7} \pm 0.8$	4350	$25.2^{+27.2}_{-21.7} \pm 0.3$	4360	$99.9^{+37.9}_{-23.4} \pm 0.7$
4370	$18.9^{+25.5}_{-20.1} \pm 0.0$	4380	$30.8^{+28.6}_{-22.7} \pm 0.2$	4390	$35.0^{+33.8}_{-27.4} \pm 0.5$
4395	$22.9^{+26.4}_{-20.0} \pm 0.5$	4400	$-11.5^{+20.3}_{-17.5} \pm 0.3$	4410	$58.1^{+40.1}_{-26.8} \pm 2.5$
4420	$86.1^{+40.9}_{-34.2} \pm 4.1$	4425	$28.7^{+26.1}_{-19.2} \pm 1.3$	4430	$74.2^{+41.2}_{-33.8} \pm 3.3$
4440	$55.3^{+32.3}_{-25.7} \pm 2.3$	4450	$4.6^{+28.2}_{-23.2} \pm 0.2$	4460	$91.1^{+8.0}_{-40.8} \pm 2.9$
4480	$30.7^{+26.7}_{-20.2} \pm 1.2$	4500	$28.8^{+27.3}_{-20.5} \pm 1.6$	4520	$25.4^{+25.8}_{-17.4} \pm 1.2$
4540	$73.6^{+32.5}_{-27.0} \pm 3.1$	4550	$39.3^{+24.2}_{-19.2} \pm 1.6$	4560	$10.1^{+19.0}_{-14.6} \pm 0.4$
4570	$42.5^{+27.0}_{-21.3} \pm 1.5$	4580	$3.8^{+16.2}_{-14.7} \pm 0.1$	4590	$6.8^{+18.1}_{-12.0} \pm 0.2$

Systematic uncertainty

- Simple event selections. The mass windows are defined with data and very loose.
- Tracking and PID, 1% for each track.
- Branching fraction of $D_s \to \phi\pi \to K^+K^-\pi$, 4.5% from PDG
- No perfect way to parameterize the line-shape, so the systematic uncertainty is large, take the difference in latest two iterations as systematic uncertainty. Dominant one.

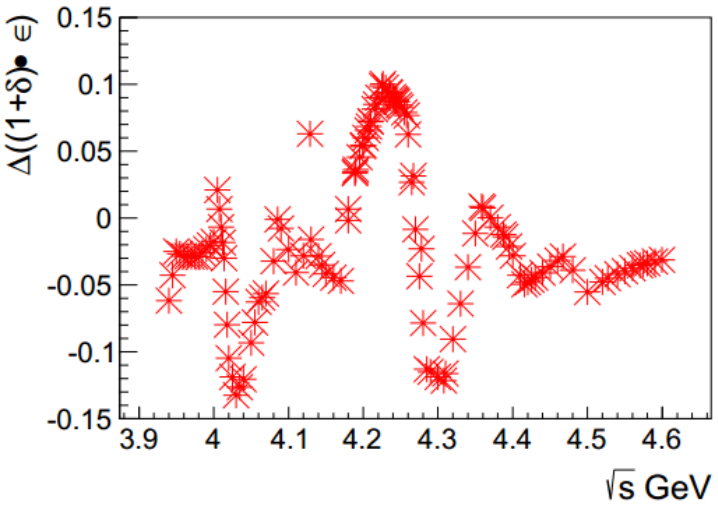

Summary

- Cross sections of $e^+e^- \to D_s^+ D_s^-$ are measured from 3.94 to 4.60 GeV with high precision.
- Clear $\psi(4040)$ signal is observed, the line-shape is not symmetric.
- A dip around 4.22 GeV is observed. With the threshold of $D_s^* D_s^*$ open, the cross section increased.
- Enhancements around 4.27 and 4.42 GeV are observed.
- Too complicated cross section distribution, so the systematic uncertainty of parameterization is large.

Thanks for your attention.
Your comments are more than welcome.